Winter 2020

Physiological and predicted metagenomic analysis of soil aggregate microbial communities under different tillage regimes

Lukas Bernhardt
University of New Hampshire, Durham

Physiological and predicted metagenomic analysis of soil aggregate microbial communities under different tillage regimes

BY

LUKAS BERNHARDT

B.S. Ecology, West Chester University of Pennsylvania, 2015

THESIS

Submitted to the University of New Hampshire

in Partial Fulfillment of

the Requirements for the Degree of

Master of Science

in

Natural Resources

December, 2020

This thesis was examined and approved in partial fulfillment of the requirements for the degree of Master of Science in Natural Resources by:

Thesis Chair: Dr. Jessica Ernakovich, Assistant Professor of Natural Resources & The Environment

Dr. Stuart Grandy, Professor of Natural Resources & The Environment

Dr. Richard Smith, Associate Professor of Natural Resources & The Environment

On: 12/4/2020

Approval signatures are on file with the University of New Hampshire Graduate School.

Acknowledgements

I would like to start by thanking the New Hampshire Agricultural Experiment Station for funding and making this project possible. Thank you to the members of my committee. Rich Smith for allowing me to work in the experimental tillage plots at Kingman Farm and for guidance in multivariate statistics. Stuart Grandy for acting as my stand in advisor during the summer of 2019. I would like to thank all who were responsible for on the ground and in the lab assistance. Bennet Thompson for helping in last minute soil sampling. Drew Ernakovich for your help in all things lab logistics. Nate Blais for assisting with DNA extractions and abiotic analyses. Kevin Geyer for showing me the ropes with carbon use efficiency. A special thanks to the Frey and Grandy Labs, especially Mel Knorr who always had time to help me with my many "quick questions". To my James Hall cohort, this experience would not have been nearly as fun without your friendship and support.

A big thanks to members of the Ernakovich Lab. Jess Mackay for helping with experimental design and analysis. Sean Schaefer for the puns and always being down to talk science. A huge thank you to Stacey Doherty for input into experimental design, data analysis and for keeping me grounded when things were particularly stressful. Lastly, I would like to thank Jessica Ernakovich for her unwavering support of my scientific creativity. I would not be here at the end of my Master's without her sensitivities to the needs of her advisees as both people and scientists.

Table of Contents

List of Tables

List of Figures

Abstract

Physiological and predicted metagenomic analysis of soil aggregate microbial communities under different tillage regimes

By

Lukas Bernhardt

University of New Hampshire

Soils are spatially heterogeneous environments, and the distribution of microorganisms and carbon is organized at the scale of millimeters in soil aggregates. The physio-chemical environment within macroaggregates and microaggregates differ, which may lead to the selection of microbial communities with different survival and growth strategies- here termed life history strategies. Using an aggregate scale survey of microbial communities in agricultural soils, I show that soil aggregates harbor distinct communities with life history characteristics that align with the Yield, Acquisition, Stress tolerator framework (Y-A-S). Soils collected from an eight- year tillage experiment were isolated into four aggregate size classes and physiological measurements of enzyme activity, multiple substrate induced respiration, and carbon use efficiency were conducted to reveal tradeoffs in community resource allocation. Carbon and nitrogen acquiring enzyme activity was highest in macroaggregates >2mm and this was negatively correlated with carbon use efficiency, which is consistent with an Acquisition- Yield strategy tradeoff. Carbon use efficiency was highest in microaggregate communities. Substrate induced respiration revealed that aggregate microbial communities showed patterns of carbon substrate preference across aggregate size class; however, these patterns were not consistent with

the Y-A-S framework. Community stress tolerance was assessed using predictive metagenomics which revealed an enrichment in genes consistent with a Stress tolerator strategy in microaggregates <0.25mm. Together, these findings show that understanding the role of the soil physical environment in shaping microbial life histories may help us to predict how agricultural management affects the fate of carbon in soils.

1. Introduction

Microorganisms regulate carbon cycling in soils which has large implications for ecosystem health (Kallenbach et al., 2016). Soil carbon stabilization is largely the result of microbial processing of organic matter via incorporation into new microbial biomass, production of extracellular byproducts, or necromass (Kallenbach et al., 2015; Prommer et al., 2020). As such, carbon cycle models have begun incorporating microbial physiology in order to better predict the fate of soil carbon globally (Allison and Goulden, 2017; Wieder et al., 2015, 2013). However, these models represent differences in microbial physiology through tradeoffs that exist across two traits (growth rate and yield), which may be insufficient to capture the fate of carbon given the complexity of the soil environment (Anthony et al., 2020). Emerging frameworks have been proposed that incorporate a wider range of microbial traits that may help us better predict microbial response to environmental conditions and ecosystem level outcomes (Krause et al., 2014; Malik et al., 2020).

Life history frameworks provide a foundation for the functional classification of microorganisms based on traits that increase fitness in response to specific environmental constraints. These frameworks reduce the vast phylogenic diversity of microbes into meaningful functional groups from which we can make predictions about ecosystem processes (Wallenstein and Hall, 2012). Microbial access to resources is limited and thus, investment of these resources comes with a cost. The Y-A-S life history framework proposed by Malik et al., 2020 hypothesizes that tradeoffs exist between microbial allocation of carbon resources towards **Y**ield (measured as new microbial biomass), resource **A**cquisition, and **S**tress tolerance. Adapted from Grime's **C**ompetitor, **S**tress tolerator, **R**uderal framework which explains the life history

strategies of plants across biomes (Grime, 1977), the Y-A-S framework centers around the emergence of microbial strategies due to resource limitation and stress (Malik et al., 2020). Yield strategists maximize the proportion of resources allocated to biomass versus total resources consumed in environments free of resource limitation. Environments where resources are scarce may favor Acquisition strategists with metabolic machinery optimized for the uptake of readily available resources (i.e. simple sugars and organic acids) or for the breakdown of complex polymers (Malik et al., 2020). Stress tolerators may invest resources into survival mechanisms such as the maintenance of cell membrane integrity or DNA repair (Guan and Liu, 2020) at the expense of growth or nutrient acquisition (Schimel et al., 2007).

Tradeoffs in resource allocation can be elucidated by measuring microbial physiological processes such as building new biomass, breaking down substrates, and the uptake of simple carbon molecules (Malik et al., 2019; Ramin and Allison, 2019). Microbial yield is the fraction of resources put towards producing new microbial biomass versus total resources consumed. Microbial carbon use efficiency is best suited to represent yield because it measures the proportion of carbon allocated to growth versus carbon lost as respiration. Community investment into resource acquisition is often measured by potential enzyme activity (Malik et al., 2019; Ramin and Allison, 2019). However, this analysis only captures the breakdown of complex polymers which is just one part of the total acquisition process. Therefore, it is also important to study the final steps of resource acquisition, the uptake of simple carbon compounds. Substrate induced respiration tools such as BIOLOG or MicroResp™ can be used to measure community response to a number of readily available carbon substrates (Campbell et al., 2003). In conjunction with enzyme activity, multiple substrate induced respiration offers a

complementary look into microbial resource acquisition, by measuring the breakdown of complex compounds and uptake of the final products respectively (Moscatelli et al., 2018).

Few studies have combined genomic tools with measurements of microbial community physiology to infer life history strategies in microbial communities. However, genomic markers can add evidence in support of emerging life history strategies (Malik et al., 2020). For example, carbon use efficiency may be correlated with genome size (Saifuddin et al., 2019) and 16S rRNA copy number (Pold et al., 2020; Roller et al., 2016) which may provide evidence for Yield strategists. Evidence for resource Acquisition strategists may be supported by the presence of genes encoding for the production of enzymes such as glycoside hydrolases or membrane transporters with affinity for simple substrates (Malik et al., 2020; Wood et al., 2018). Although, microbial response to stress will depend on the abiotic conditions encountered, genes relating to cell wall biosynthesis and maintenance confer stress under a wide range of conditions (Wood et al., 2018). Combining physiological measurements with predicted metagenomic features may allow us to gain novel insights into microbial life history strategies.

The productivity and overall function of agricultural ecosystems relies on microbially mediated carbon cycling in soils which is crucial for maintaining crop productivity (Lal, 2010) and overall ecosystem function. The Y-A-S life history framework may provide us with conceptual tools for understanding how differences in resource allocation among microbial functional groups affect the fate of carbon in soils. Thus, applying this theory in the context of agricultural systems may help to predict how carbon is stored, which can provide a path towards improving agricultural sustainability. Further, agricultural soils provide a unique system of study for testing the applicability of the Y-A-S framework because management decisions interact with factors that may alter life history such as access to carbon, and the physical environment in

which microbes reside. For example, tillage has been shown to reduce carbon relative to untilled soils resulting from a loss of carbon rich macroaggregates and an increase in the proportion of carbon depleted microaggregates (Six et al., 2000). Although, life history frameworks have been applied previously to soil microbial communities in agricultural systems, these studies were conducted on bulk soil (Malik et al., 2019; Schmidt et al., 2018). We may be able to gain additional insights by applying the Y-A-S framework— and life history strategies broadly— at the scale of aggregates because these microhabitats are unique environments with distinct physical and chemical characteristics (Six et al., 2004; Bach et al., 2018).

Soils are comprised of a complex matrix of aggregates, tightly bound minerals and organic matter that form the fundamental units of soil (Wilpiszeski et al., 2019). Soil aggregation operates within a hierarchy of size (Tisdall and Oades, 1982). Macroaggregates (>0.25mm diameter) are composed of microaggregates, held together by a tangle of fungal hyphae and roots (Tisdall and Oades, 1982). Macroaggregates are heavily influenced by agricultural practices, due to the transient nature of the binding agents holding them together. Microaggregates (<0.25mm in diameter) form within macroaggregates due to persistent organo-mineral associations (Tisdall and Oades, 1982). Aggregates of varying sizes differ in pore structure (Bailey et al., 2013; Foster, 1988), oxygen availability (Sexstone et al., 1985), and carbon chemistry (Davinic et al., 2012; Trivedi et al., 2017). As a result, aggregates support microbial communities with distinct compositions (Bach et al., 2018; Bailey et al., 2013; Trivedi et al., 2015, 2017a). However, it is unclear why communities differ between aggregates. Life history frameworks may provide us with predictive tools to understand this relationship between microbial community composition and microhabitats in soil (Anthony et al., 2020).

In this study, I employed a combination of physiological measurements and predictive metagenomic tools to explore whether there are emergent microbial life history strategies that exist within aggregates of different size classes in an agricultural system. The overarching hypothesis for this study is that aggregates of different size classes harbor communities that can be classified into life history strategies within the Y-A-S life history framework. I hypothesize that aggregates >2mm will harbor organisms that employ a Yield strategy, due to a greater amount of microbially available carbon in larger aggregate size classes. I hypothesize that aggregates <0.25mm will harbor Stress tolerators, due to low pore connectivity in microaggregates which may lead to both osmotic and oxidative stress. I hypothesize that aggregates 0.25mm-2mm will harbor acquisition strategists due to increasing carbon complexity that necessitates enzymatic breakdown. Lastly, I hypothesize that the relationships between aggregate size and life history strategy will persist regardless of agricultural management (tillage). This is based on previous studies which have found that aggregates harbor distinct microbial communities regardless of agricultural management (Trivedi et al., 2017). To address these hypotheses, I sampled soil from an 8 year tillage experiment and isolated aggregates of four sizes (<0.25mm, 0.25mm-1mm, 1mm-2mm, and >2mm) using an optimal moisture sieving technique (Bach and Hofmockel, 2014). Multiple substrate induced respiration, enzyme activity, and carbon use efficiency were measured to classify aggregate communities into the Y-A-S framework based on physiology. Metagenome prediction via PICRUSt2 (Douglas et al., 2020) was used to measure microbial Stress tolerance and to add support to the Yield- Acquisition classifications. Hypothesized physiological and metagenomic results are outlined in Figure 1.

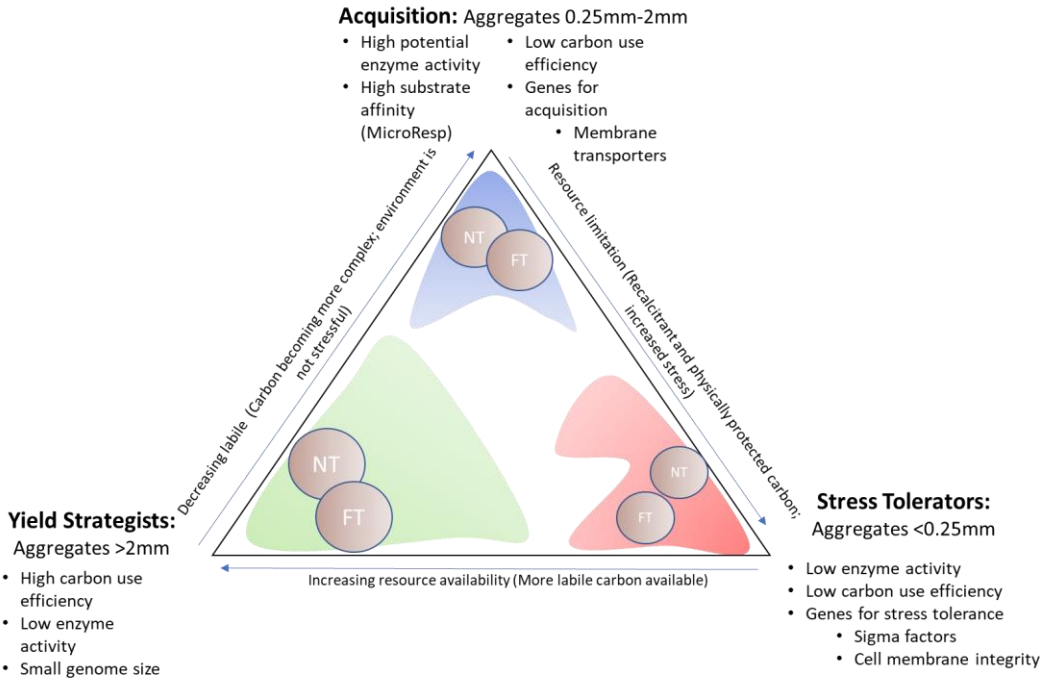

Figure 1: Conceptual diagram outlining the hypotheses above, elaborating on expected physiological and genomic traits in each life history class. Size of the circles represents relative aggregate size. NT= no-till; FT= full-till. Adapted from (Krause et al., 2014)

2. Materials and Methods

2.1 Site description and sampling

Soils were collected from a long-term tillage experiment at the University of New Hampshire Kingman Farm in Madbury, NH in May 2019 (N 43°10.333', W 70°56.307'). Prior to establishment of the experiment in 2012, the site was converted from standard management practices (full-till; corn-soy rotation; planted with pesticide coated seeds) in 2013 to a tillage experiment with three till intensities, including the two sampled for this study; full- till (FT) and no- till (NT). In 2016, paired plots planted without pesticide coated seeds were included with each tillage treatment which resulted in a fully factorial design between tillage and seed type replicated across four blocks. Full-till plots were managed by full inversion of the soil to 30 cm depth with a moldboard plow followed by preparation of the seed bed with shallow disking. Pesticide seed treated plots were sampled however, did not affect any of the metrics included in this study and have been retained as additional tillage replicates to increase statistical power. Additional management activities in these plots included yearly applications of glyphosate both before and after planting and annual application of liquid manure from the University of New Hampshire dairy to maintain soil fertility. Plots were planted under corn in 2018, the season preceding sampling for this study. Plots are 26 meters x 6.1 meters, replicated across four blocks separated by 12.2-meter unmanaged strips (Figure S1).

Soils were sampled in late May 2019 prior to spring tillage and glyphosate application to minimize the potential effects of recent disturbance. The two full-till (FT) and two no-till (NT) plots from each block were sampled using a slide hammer coring device to a depth of 10 cm. Twelve soil cores were collected across each tillage treatment plot and composited in one bag. This sampling design yielded 8 replicates of each tillage treatment. Samples were stored on ice

and transported to 4 °C within 6 hours. Prior to aggregate isolation, soils were passed through an 8 mm sieve to facilitate the removal of roots and large rocks.

2.2 Aggregation isolation and sample storage:

Aggregates of 4 different size classes (<0.25mm, 0.25mm-1mm, 1mm-2mm, and >2mm) were isolated using an optimal moisture sieving technique (Bach and Hofmockel, 2014). This method consistently separates aggregates while minimizing disturbance to the soil, making measurements of microbial physiology more reflective of *in situ* conditions than the disturbance of soil processing (Bach and Hofmockel, 2014). Soils were dried for one week in covered autoclaved tins using desiccant beads to reduce gravimetric water content to 0.1g H_2O g $soil^{-1}$ (optimal moisture for isolation). Aggregate size classes were isolated by placing repeated batches of 375 g dried soil on stacked sterile sieves with mesh openings of 250 um, 1 mm, and 2mm affixed to a vibratory sieve shaker (40 amps for 2.5 minutes; Retsch AS200). The vibratory sieve shaker was used to minimize disturbance to the aggregates while still facilitating consistent aggregate separation similar to the procedure of Bach and Hofmockel, 2014. Aggregate size fractions were weighed to determine the mass of soil in each size class and were retained for further analyses if > 97% recovery of total soil mass was met. A subset of each aggregate size class was dried for analysis of total carbon, total nitrogen, pH and electric conductivity (EC). A second subset of 3 g was frozen upon isolation at -80 ^oC for DNA extraction and community classification. A third subset was frozen at -20 ^oC for enzyme analysis. The remainder of each size class was stored at 4 ^oC for physiological analysis via MicroResp™ and carbon use efficiency. All analyses for this study were conducted within 3 months of initial sampling.

2.2 Aggregate abiotic classification

Aggregate pH and EC were determined with a soil to water ratio of 1:5 using Accumet Basic AB15 and Accumet Basic AB30 (Fisher Scientific, Hampton, NH) probes respectively. Field moisture content was measured by drying 10g of soil at 105ºC for 3 days and recording mass loss. Water holding capacity (WHC) was determined by wetting approximately 50g of each aggregate to capacity and measuring moisture content (as above) after draining for 48 hours. Total carbon and total nitrogen were measured by elemental combustion analysis (Costech EC4010, Valencia, CA).

2.3 Bacterial and fungal community analysis

DNA extractions were performed using the Qiagen DNeasy PowerSoil Kit (Venlo, Netherlands), following the manufacturer's protocol with slight modifications to maximize DNA recovery from samples. Modifications are as follows (from Geyer et al., 2019): 1) all supernatant was retained in each step 2) all centrifuge times were increased to 1 min to ensure separation of DNA from co-extracted materials, 3) the final spin filter received a 600 ul 96% ethanol rinse and 4) volumes of reagents were adjusted to maintain extractant:supernatant ratio. DNA concentrations were quantified using the PicoGreen fluorescence assay (Quant-iT^{TM} PicoGreen Kit, Thermo Fisher, Germany) on a Biotek Synergy HT microplate reader (VT, USA).

Bacterial and fungal community composition were analyzed through amplicon sequencing of ribosomal RNA (rRNA). The V4 region of the bacterial 16S gene was targeted using primers 515f-926r and primers ITS1F/ITS2 of the internal transcribed spacer were used to target fungal communities (Walters et al., 2016). Amplification of DNA was conducted using polymerase chain reaction (PCR). For each PCR reaction 0.7 ul of both forward and reverse

primer (5mM) were combined with 6 ul DreamTaq HotStart (Thermo Scientific, Waltham, MA), 2 ul (1ng/ul) template DNA and 2.6 ul dH_2O. The conditions of amplification were as follows: enzyme activation at 95 °C for 3 minutes; 35 cycles of denaturing at 95 °C for 30 seconds; annealing at 55 °C for 30 seconds, and extension at 72 °C for 60 s, followed by a final extension at 72 °C for 12 min. Amplification of the desired regions was confirmed via gel electrophoresis. PCR product containing 16S and ITS amplicons were sequenced at the UNH Hubbard Center for Genome Studies (University of New Hampshire, Durham, NH) on the Illumina HiSeq 2500 platform (Illumina, San Diego, CA). Average read counts per sample for 16S and ITS amplicons were 44895 and 89525 respectively.

Bioinformatic analysis of the bacterial and fungal sequences were conducted in QIIME2 version 2019.4 (Bolyen et al., 2019). For 16S sequences, primers were removed using Cutadapt (Martin, 2011) and sequences were trimmed and denoised using DADA2 (Callahan et al., 2016). Taxonomy was assigned by comparing reads against the GreenGenes database (version 3.8.19). Sequences were rarefied to 4500 reads and clustered to 97% similarity as operational taxonomic units (OTU's). Following rarefication, 5 samples were dropped from analysis due to low read counts. For ITS sequence analysis, primers and conserved regions were removed using ITSxPress (Rivers et al., 2018). The remaining steps follow the 16S methods outlined above through DADA2. ITS taxonomy was assigned using the UNITE database (Nilsson et al., 2019) and sequences were rarefied to 22000 reads.

Community weighted genome size and rRNA copy number for the bacterial community were predicted via ancestral state reconstruction in R (version 3.6.3) (R Core Team, 2018). Briefly, 16S sequences were placed on a reference phylogenetic tree described in Gravuer and Eskelinen, 2017 using pplacer (Matsen et al., 2010). Function phyEstimate() in the picante

package (version 1.8.2) (Kembel et al., 2010), was used to estimate genome size and rRNA copy number for each 16S sequence based on the phylogenetic distance from a reference sequence with known genome size and rRNA copy number. OTU relative abundance was corrected for rRNA copy number using the script from (Kembel et al., 2012) and community weighted mean trait values were calculated using the FD package (Laliberté et al., 2014).

Functional gene prediction for bacterial communities was performed using Phylogenetic Reconstruction of Unobserved Traits 2 (PICRUSt2) (Douglas et al., 2020). PICRUSt2 works by predicting the metagenomic composition of 16S amplicons using relative organisms for which there is are fully annotated genomes as a reference. Functional gene abundance measured as KEGG orthologs (KO) was predicted via hidden-state prediction (Louca and Doebeli, 2018). Fit of the reference database was validated by weighted NSTI values which indicate the average phylogenetic distance from query sequences to known reference sequence (Supplementary Table 1). The KEGG database contains information on experimentally characterized gene function. This function can be mapped onto microbial OTU's using orthologous genes (genes with the same function across species) found in both the database and OTU.

2.4 Community physiological profiling by substrate induced respiration (SIR), enzyme activity, and carbon use efficiency

Multiple substrate induced respiration was measured using the MicroResp™ system (Campbell et al., 2003) with seven substrates representing various chemical groups: (L-Arginine, L-Lysine (amino acids); D-(+)Trehalose, D-(+)Glucose, L-(+)Arabinose (carbohydrates); and Citric acid, L-Malic acid (carboxylic acids) and a water control (Milli-Q H_2O). Aggregates were weighed into deep-well microplates (Abgene™ 96 Well 1.2mL Polypropylene Deepwell Storage Plate), wetted to 55% WHC and pre-incubated covered for 5

days at 25 ºC. Three replicates for each aggregate size class were included with an average weight per well of 0.362 g. Following pre-incubation, substrates were added (30 mg g^{-1} total soil water) to the wells and plates were fitted with the MicroResp^{TM} rubber gasket covered with a CO_2 colorimetric detection plate. Detection plates were prepared containing a creosol red indictor dye which changes color in the presence of CO_2. A calibration curve for absorbance versus headspace CO_2 concentration was calculated by incubating 4 different soils with 0µl, 50µl and 200µl of glucose solution (0.2mg/µl) for 6 hours and measuring absorbance and headspace CO_2 concentration (Campbell et al., 2003). Absorbance of the detection plate was measured following a 6-hour incubation at 25 ºC. Total CO_2 production per substrate was corrected for biomass by subtracting H_2O induced respiration and analyzed as ug C-CO_2g dry-$soil^{-1}$ hr^{-1}. To compare microbial substrate preferences, relative substrate use for each aggregate size class was calculated by dividing substrate induced respiration by the total induced respiration across all substrates.

The potential enzyme activity of five hydrolytic enzymes was assessed for each aggregate size class: β-glucosidase (BG), N-acetyl-B-D-glucosaminidase (NAG), Leucine-7-aminopeptidase (LAP), cellobiohydrolase (CBH), and acid phosphate (PHOS), following protocols adapted from (German et al., 2011; Saiya-Cork et al., 2002). Fluorescent standards (MUB and MUC) and substrates (BG, CBH, NAG, LAP, PHOS) were made within one week of conducting analysis and stored frozen at -20 ºC. V-max tests were conducted on bulk soils from these sites in 2018 and optimal substrate concentration and incubation time were described in Table 1.

Table 1: Concentrations of substrates and incubation times for enzyme assays. Data taken from V-max test performed on the same soils September 2018

Enzyme	Substrate	[Conc.] uM	Incubation Time (hours)	Incubation Temperature (°C)
BG	4-MUB-B-D-glucopyranoside	600	4	25
CBH	4-MUB-B-D-cellobioside	600	4	25
NAG	4-MUB-N-acetyl-B-D-glucosaminide	600	4	25
LAP	Leucine-7-amino-4-methylcoumarin	900	3	25
PHOS	4-MUB-phosphate	900	3	25

For each assay, a sample control, buffer control, and substrate control were performed as well as 16 replicate wells of each aggregate size class by enzyme combination. Briefly, 1 gram of each aggregate size class was combined with 125 mL of 50mM sodium acetate buffer (pH 6.47) to form a slurry. While stirring, the slurry was pipetted into wells using a multichannel pipette. Substrates were added to assay wells and time was recorded for the start of the incubation. After the desired incubation time (Table 1), the plates were read on a Biotek Synergy HT microplate reader at 360 nm and 460 nm excitation and emission wavelengths respectively. Total enzyme activity corrected for differences in microbial biomass was analyzed (umol enzyme activity unit biomass^{-1} h^{-1}).

Carbon use efficiency was measured using the ^{18}O Water tracing method from Geyer et al., 2019. Aggregates were pre-incubated at 40% WHC and 25 ^{o}C for five days, following which, 0.4 g of each aggregate was weighed into two microcentrifuge tubes. For each sample, one tube received enriched (~97 at%) ^{18}O-water diluted with unlabeled deionized water for a total enrichment of 20 at%. The second tube received natural ^{18}O abundance deionized water as a control. Microcentrifuge tubes were inserted into 50 mL amber vials, capped with rubber septa, and flushed with CO_2-free air for 10 minutes at 10 psi. Aggregates were incubated at 25 ^{o}C for 24 hours following which, 3 mL of vial headspace was sampled via syringe and injected into a LI-COR 6252 benchtop CO_2 analyzer (Lincoln, NE) calibrated against a 5-point standard curve

of known CO_2 concentrations. Aggregates were immediately moved to a -80^oC freezer to await DNA extraction. DNA Extracts were dried for 24h at 60^oC in 8x5mm silver capsules. Dried extracts were spiked with 100 µL diluted salmon sperm (1.0 µg $µL^{-1}$) to bring total oxygen mass within a detectable range. Samples were stored in a desiccator prior to shipment to UC Davis Stable Isotope facility for δO^{18} quantification via temperature conversion elemental analysis (PyroCube Elementar Analysensysteme GmbH, Hanau, Germany). Due to machine error during O^{18} quantification, CUE analysis includes 33 datapoints spanning all 4 aggregate size classes and both tillage treatments (<0.25mm, n= 8; 0.25mm-1mm, n= 7; 1mm-2mm, n= 8; >2mm, n= 9). All other physiological analyses include 64 datapoints (n= 16 per aggregate class).

Microbial biomass was calculated via the substrate induced respiration method of Anderson and Domsch, 1978 with modification. Microbial biomass can be calculated from the following conversion: 1 µl CO_2 h^{-1} glucose induced respiration corresponds to 40 µg microbial biomass C over short incubations (1-3 hours) at 22 ^oC (Anderson and Domsch, 1978). Glucose induced respiration from MicroResp™ measurements (µl C-CO_2 g^{-1} dry soil h^{-1}) were converted to microbial biomass C (µg C g^{-1} dry soil h^{-1}) using the equation from Anderson and Domsch, 1978 (µg biomass C= (µl CO2 g^{-1} dry soil h^{-1}) 40.04 + 0.37). Soils for biomass calculations were incubated at 25 ^oC for 6 hours rather than 22 ^oC for 1-3 hours. As such, my incubation conditions were modifications from the original Anderson and Domsch method and may represent an overestimation of microbial biomass. However, I expect that these modifications would affect my samples uniformly, and thus the relationship between treatments would be maintained. In order to validate measurements of microbial biomass, linear regression was performed to test the relationship between total carbon and microbial biomass as these two measurements are highly correlated (Supplementary Figure 2). Total carbon and microbial biomass were strongly

correlated (R^2= 0.39; $p < 0.001$), although, not as strongly as previously cited in the literature (Anderson and Domsch, 1989). Thus, to further increase confidence in biomass calculations, linear regression was performed to test the relationship between soil DNA (ng g^{-1} dry soil) (Supplementary Figure 3). Calculations for CUE follow equations from Geyer et al., 2019 adapted from Spohn et al., 2016.

2.5 Data processing and statistics:

Statistical analyses were conducted in R (version 3.6.3) (R Core Team, 2018). Normality and homoscedasticity of all data were assessed using Shapiro-Wilks and Levene's test respectively. pH did not meet assumptions of normality and was log transformed prior to analysis. Differences in abiotic characteristics among aggregates and between tillage treatments were determined using two- way analysis of variance (ANOVA). Post-hoc Tukey HSD tests were performed to determine which aggregate size classes were driving statistically valid differences as determined by ANOVA. Statistical differences between tillage treatments and aggregate size classes, were determined using permutational multivariate analysis of variance (PERMANOVA) in the 'vegan' package (Oksanen et al., 2019) for SIR, and enzyme activity. Permutations were constrained by block to account for random effects. As tillage significantly impacted both SIR and enzyme activity, individual substrates and enzymes across aggregate size classes were analyzed separately for NT and FT treatments via ANOVA. All enzyme activity, arginine, glucose, lysine and water induced respiration were log transformed prior to analysis to meet the assumptions of normality.

Differences in microbial communities and predicted gene composition were visualized using non-metric multidimensional scaling (NMDS) with Bray-Curtis dissimilarity.

PERMANOVA was used to confirm differences across aggregate size classes and tillage treatment. Permutations were constrained by experimental block to account for random effects. Genome size and rRNA copy number were analyzed using two-way ANOVA to test for the effects of tillage and aggregate size class. KEGG orthologs were analyzed using STAMP v2.1.3 (Statistical Analysis of Taxonomic and Functional Profiles) (Parks et al., 2014) for differential abundance of predicted genes across aggregate size classes using White's non-parametric t-test with Benjamini-Hochberg FDR correction. False discovery rate (FDR) was set at 0.05.

3. Results

3.1 Aggregate distribution

The proportion of aggregates <0.25mm, 1mm-2mm, and >2mm were significantly different between no-till and full-till treatments (Figure 2). This was driven largely by the reduction in macroaggregates due to tillage. The proportion of aggregates >2mm was 3 and 2 times greater than aggregates <0.25mm in no-tilled and full-tilled treatments respectively. Within no-till treatments, the proportion of aggregates in each size class differed significantly ($F= 162.1$; $p < 0.001$). <0.25mm aggregates were least abundant under no-till treatment constituting just 11.6 % ± 1.01 % of total aggregate composition. In full-till treatments, aggregates <0.25mm and 1mm-2mm differed significantly from aggregates 0.25mm-1mm and >2mm ($F= 36.71$; $p < 0.001$) (Figure 2).

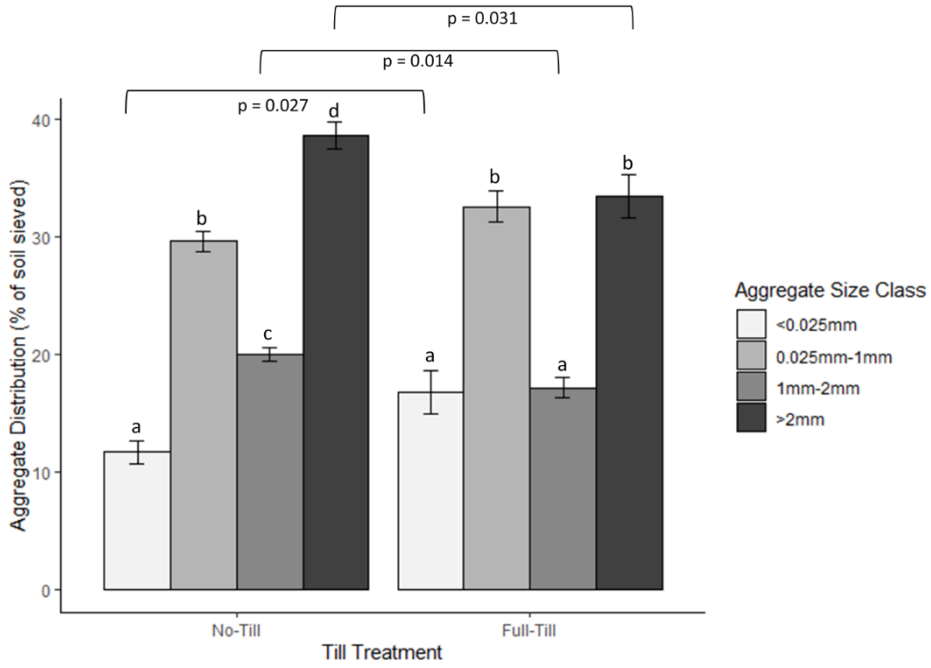

Figure 2: Aggregate size class distribution in no-till (left) and full-till (right) treatments. Lower case letters denote significance within tillage treatment. p-values denote significant differences between aggregates within the same size class under no-till and full-till. p-values and significance within tillage treatment determined using two-way ANOVA and Tukey HSD post-hoc test.

3.2 Aggregate Abiotic Properties

Total carbon did not vary across aggregate size classes within either tillage treatment ($F= 1.917$; $p > 0.05$). Under no-till, total nitrogen was significantly higher in aggregates < 0.25mm compared to the 0.25mm-1mm and 1mm-2mm size classes; however, total nitrogen did not differ between the <0.25mm and >2mm size class (Table 1; (Table 1; $F= 4.74$; $p < 0.01$). Water holding capacity was highest in the no-till treatment ($F= 42.19$; $p < 0.001$) and differed by aggregate size class ($F= 23.645$; $p < 0.001$). Under both tillage treatments, water holding capacity was highest in the smallest aggregate size class and decreased with increasing aggregate size (Table 1). Both pH ($F= 7.12$; $p < 0.01$) and electric conductivity ($F= 29.54$; $p < 0.001$) were significantly higher under the no-till treatments but did not vary by aggregate size class. The no-till and full-till treatments had a mean soil pH of 6.63 ± 0.091 and 6.34 ± 0.059 respectively.

Table 2: Mean and standard error of soil chemical, physical, microbial community properties for no-till and full-till treatments in each aggregate size class. Basal respiration calculated from water induced respiration (MicroResp™). Bolded letters denote significant differences between aggregate size classes within tillage treatment analyzed by ANOVA and Tukey HSD post hoc test. Treatments sharing the same letter were not significantly different.

	<0.025 mm		**0.025 mm-1 mm**		**1 mm- 2 mm**		**>2mm**	
Environmental and Microbial Metrics	NT	FT	NT	FT	NT	FT	NT	FT
Chemical								
pH	6.52 ± 0.11	6.28 ± 0.13	6.63 ± 0.16	6.37 ± 0.13	6.93 ± 0.28	6.44 ± 0.11	6.46 ± 0.095	6.3 ± 0.11
EC	32.72 ± 2.89	21.25 ± 2.17	31.07 ± 3.41	18.29 ± 2.15	26.04 ± 2.60	18.97 ±1.86	29.97 ± 2.94	20.18 ± 2.67
Total C (g carbon g dry soil^{-1})	0.027 ± 1.6e-03	0.021 ± 1.1e-03	0.023 ± 1.9e-03	0.02 ± 1.4e-03	0.022 ± 1.1e-03	0.019 ± 1.4e-03	0.024 ± 1.2e-03	0.02 ± 8.0e-03
Total N (g nitrogen g dry soil^{-1})	0.0025 ± 1.4e-04**a**	0.0019 ± 8.77e-05	0.0021 ± 1.4e-04**b**	0.0018 ± 1.02e-04	0.002 ± 6.7e-05**b**	0.0017 ± 1.13e-04	0.0022 ± 8.82e-05**ab**	0.0018 ± 6.68e-05
C:N	10.53 ± 0.13	10.48 ± 0.12	10.9 ± 0.23	10.69 ± 0.21	10.85 ± 0.22	10.95 ± 0.19	10.87 ± 0.20	10.68 ± 0.12
Microbial Biomass (ug C-mic g^{-1} dry soil)	332.15 ± 41.9	253.67 ± 27.44	315.8 ± 12.9	213.41 ± 21.76	274.64 ± 20.65	172.46 ± 21.97	200.17 ± 14.25	132.81 ± 11.65
Physical								
WHC (g H_2O g dry soil $^{-1}$)	0.73 ± 0.015**a**	0.67 ± 0.018**a**	0.65 ± 0.018**b**	0.57 ± 0.018**b**	0.58 ± 0.02**bc**	0.51 ± 0.019**bc**	0.52 ± 0.02**cd**	0.46 ± 0.02**c**
Absolute Enzyme Values								
PHOS (nmol h^{-1}g^{-1})	1002.81 ± 318.71	734.04 ± 79.50**a**	813.86 ±168.85	511.45 ±113.51**b**	753.41 ±140.2	676.64 ±98.16**b**	613.56 ±81.87	374.45 ±31.91**b**
BG (nmol h^{-1} g^{-1})	401.17 ± 76.83	228.09 ± 33.09	370.17 ±47.28	199.76 ±32.60	322.29 ±43.02	249.5 ±41.24	365.67 ±48.41	151.99 ±13.67
NAG (nmol h^{-1} g^{-1})	98.88 ± 15.28	57.73 ± 8.88a	94.94 ±8.302	54.63 ±7.66	84.01 ±11.11	65.46 ±9.64	101.12 ±5.28	48.57 ±7.61
LAP (nmol h^{-1} g^{-1})	88.67 ± 14.94	76.64 ± 9.83	88.86 ±13.00	56.09 ±13.16	72.52 ±7.99	70.11 ±15.21	72.04 ±7.89	42.43 ±5.12
CBH (nmol h^{-1} g^{-1})	92.76 ± 16.77	40.66 ± 5.93	85.94 ±11.01	36.61 ±6.68	73.97 ±10.19	41.64 ±7.70	79.63 ±5.98	31.64 ±6.45
Substrate Induced Respiration								
Arginine (ug CO_2-C g^{-1} dry soil h-^{1})	1.25 ± 0.42	0.97 ± 0.22	1.07 ± 0.15	0.62 ± 0.17	1.28 ± 0.21	0.82 ± 0.16	0.89 ± 0.15	0.67 ± 0.15
Lysine (ug CO2-C g^{-1} dry soil h^{-1})	0.40 ± 0.15	0.23 ± 0.08	0.20 ± 0.05	0.17 ± 0.07	0.47 ± 0.07	0.25 ± 0.06	0.34 ± 0.07	0.24 ± 0.08
Citric Acid (ug CO_2-C g^{-1} dry soil h^{-1})	1.81 ± 0.33	1.13 ± 0.27	2.10 ± 0.15	1.12 ± 0.24	2.72 ± 0.11	1.81 ± 0.22	2.30 ± 0.30	1.54 ± 0.23
Malic Acid (ug CO_2-C g^{-1} dry soil h^{-1})	1.97 ± 0.56	1.25 ± 0.26	1.85 ± 0.21	0.92 ± 0.17	1.33 ± 0.14	0.74 ± 0.15	1.34 ± 0.25	1.01 ± 0.19
Trehalose (ug CO_2-C g^{-1} dry soil h^{-1})	1.69 ± 0.39	1.09 ± 0.23	1.63 ± 0.15	0.88 ± 0.14	1.44 ± 0.12	0.78 ± 0.18	1.31 ± 0.20	1.09 ± 0.16
Arabinose (ug CO_2-C g^{-1} dry soil h^{-1})	0.91 ± 0.21	0.65 ± 0.15	1.19 ± 0.18	0.54 ± 0.13	1.47 ± 0.11	0.91 ± 0.15	1.30 ± 0.16	0.86 ± 0.12
Glucose (ug CO_2-C g^{-1} dry soil h^{-1})	2.30 ± 0.50	1.78 ± 0.29**a**	2.44 ± 0.17	1.48 ± 0.19**ab**	2.30 ± 0.18	1.19 ± 0.26**ab**	1.44 ± 0.23	0.23 ± 0.12**b**
MSIR (total ug CO2-C g-1 dry soil h-1)	10.34 ± 2.44	7.1 ± 1.32	10.49 ± 0.81	5.73 ± 0.86	11.03 ± 0.77	6.5 ± 0.11	8.94 ± 1.24	6.22 ± 0.94
Basal Respiration (ugCO_2 h^{-1}g^{-1})	1.76 ± 0.19	1.32 ± 0.19	1.42 ± 0.13	1.12 ± 0.14	1.05 ± 0.11	0.92 ± 0.11	1.00 ± 0.09	0.79 ± 0.08

3.3 Microbial community composition:

Bacterial community composition differed by tillage treatment ($F= 6.89$; $p < 0.001$) and aggregate size classes ($F= 1.45$; $p < 0.01$) as determined by PERMANOVA and visualized by Non-metric Multidimensional Scaling (NMDS) (Figure 3a). However, there was no significant interaction between tillage and aggregate size class ($p > 0.05$). Shannon's and Faith's phylogenetic diversity did not vary by either aggregate size class ($F= 0.80$; $p > 0.05$) or by tillage treatment ($F= 0.91$; $p > 0.05$). Soil pH, WHC and EC correlated with the arrangement of samples in the NMDS (pH, $p = 0.004$; EC, $p = 0.006$, WHC, $p = 0.006$). Pairwise comparisons of aggregate microbial communities confirmed that bacterial composition differed between macroaggregates (>2 mm) and the <0.25 mm aggregate size class ($p = 0.018$).

Aggregates <0.25mm differed significantly from the 1mm-2mm and >2mm aggregates in fungal community composition by both tillage treatment ($F= 5.27$; $p < 0.001$) and aggregate size class ($F= 1.45$; $p < 0.01$) (Figure 3b). All environmental variables tested (pH, EC, WHC, total N, total C, C:N) were correlated with fungal community composition (pH, $p < 0.01$; EC, WHC, TN, TC, C:N, $p < 0.001$). It should be noted that experimental block was significant in shaping both bacterial and fungal microbial communities (Supplementary Figure 4). As such, PERMANOVA's were constrained by block to account for this random effect.

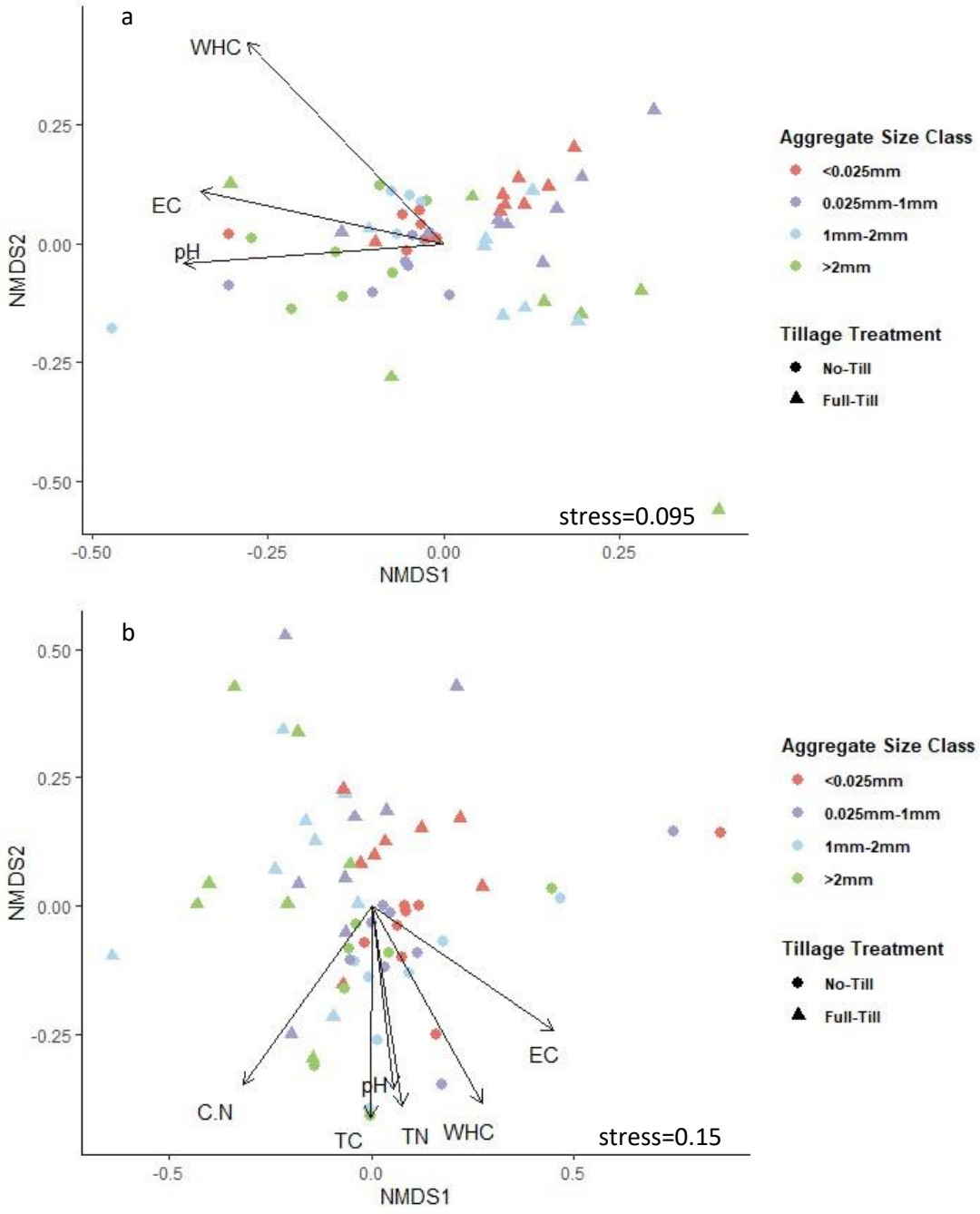

Figure 3: Microbial community composition visualized by non-metric multidimensional scaling using Bray-Curtis distance for both bacterial (a) and fungal (b) communities. Both tillage treatment and aggregate size class were significant factors in shaping community composition in both bacterial and fungal communities. Colors represent tillage treatment and point shape represents aggregate size class.

3.4 Microbial Physiology

Microbial uptake of simple carbon molecules was measured via substrate induced respiration. Seven carbon substrates were tested across three types: amino acids, carboxylic acids, and carbohydrates. Comparison of the full SIR profile via PERMANOVA revealed that both tillage ($F= 11.99$; $p < 0.001$) and aggregate size ($F= 1.77$; $p < 0.05$) impacted community response to carbon substrates. SIR response to tillage was consistently higher in no-till treatments across all 7 substrates. Total SIR respiration in no-till aggregates was 10.20 ± 0.72 µg CO_2-C g^{-1} dry soil h^{-1} while full-till aggregates respired 6.39 ± 0.52 µg CO_2-C g^{-1} dry soil h^{-1}. Although SIR was impacted by aggregate size, the relationship between respiration and size was not consistent across substrates or type (Supplementary Figure 5). To note changes in SIR in aggregate size classes, the following results are averaged across tillage. Glucose induced respiration decreased with increasing aggregate size (Figure 4g, $F= 4.73$; $p < 0.01$). Aggregates <0.25mm respired at a rate nearly twice as much as aggregates >2mm in response to glucose addition (2.04 ± 0.28 µg CO_2-C g^{-1} dry soil h^{-1} and 1.14 ± 0.15 µg CO_2-C g^{-1} dry soil h^{-1} respectively). Arabinose, also a carbohydrate, elicited an opposite response however the magnitude was much lower (Figure 4f). Microbial response to citric acid was positively correlated with aggregate size which followed the same trend as arabinose ($F= 4.301$: $p < 0.01$). Citric acid induced respiration was highest in 1mm-2mm aggregates (2.27 ± 0.17 µg CO_2-C g^{-1} dry soil h^{-1}) and lowest in aggregates <0.25mm (1.47 ± 0.22 µg CO_2-C g^{-1} dry soil h^{-1}) (Figure 4c). Total SIR was calculated by the cumulative respiration induced by all seven substrates after correcting for water induced respiration. There was no overall trend between total SIR and aggregate size (Figure 4h).

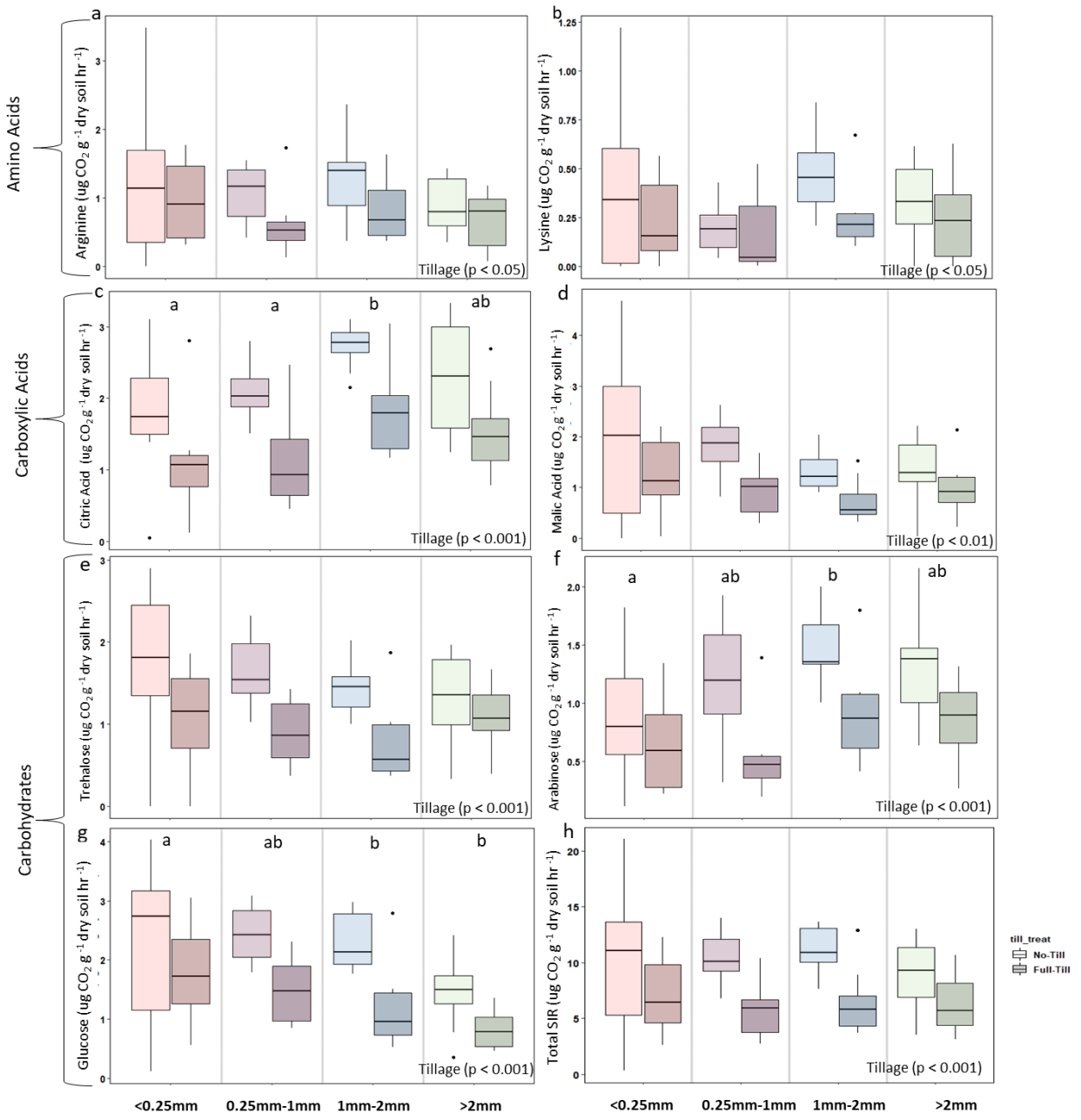

Figure 4: Boxplot showing differences in substrate induced respiration across both tillage and aggregate size class measured as µg CO_2-C g^{-1} dry soil h^{-1} (panels a-g). Panel h shows total SIR measured as the sum of respiration above the water control across all substrates. Lighter shaded boxes represent no-till treatments and darker shaded boxes represent full-till treatments. Two- way ANOVA was used to analyze the effect of tillage and aggregate size class on SIR. Tukey HSD post-hoc tests confirmed significant differences between respiration in aggregate size classes. Letters denote significant changes in SIR in aggregate size in the global model.

To understand the microbial community investment into nutrient and carbon acquisition, extracellular enzyme activity of two carbon acquiring (BG, CBH), two nitrogen acquiring (LAP, NAG), and one phosphorus acquiring (PHOS) enzymes were measured. As a result of differing microbial biomass between tillage treatments ($F= 27.92$; $p < 0.001$) and aggregate size classes ($F= 10.96$; $p < 0.001$), enzyme activity was relativized per unit biomass to minimize the confounding effects of microbial biomass on carbon and nutrient acquiring enzymes (Figure 5). The full enzymatic profile did not differ by either tillage treatment or aggregate size class when analyzed via PERMANOVA. However, when individual enzymes were analyzed, patterns began to emerge. CBH activity was significantly lower in tilled aggregates (0.21 ± 0.019 nmol activity unit biomass^{-1}) relative to no-tilled aggregates (0.32 ± 0.022 nmol activity unit biomass^{-1}) ($F= 15.662$; $p < 0.001$). Further, CBH activity increased with increasing aggregate size class ($p= 0.08$). BG activity was trending towards significance between tillage treatments ($F= 2.935$; $p= 0.09$) and aggregate size ($F=2.33$; $p= 0.083$). NAG activity was 1.5 times higher in aggregates >2mm (0.44 ± 0.033 nmol activity unit biomass^{-1}) relative to aggregates <0.25mm (0.29 ± 0.041 nmol activity unit biomass^{-1}) ($F= 5.25$ $p < 0.01$). Total N acquiring enzyme activity (sum of LAP and NAG) was significantly higher in aggregates >2mm than aggregates <0.25mm ($F= 8.43$; $p < 0.001$) (Figure 5b). Similarly, total C acquiring enzyme activity (sum of BG and CBH) was significantly higher in aggregates >2mm ($F= 7.25$; $p < 0.001$) (Figure 5a). Total enzyme activity was consistent between tillage treatments and across aggregate size classes.

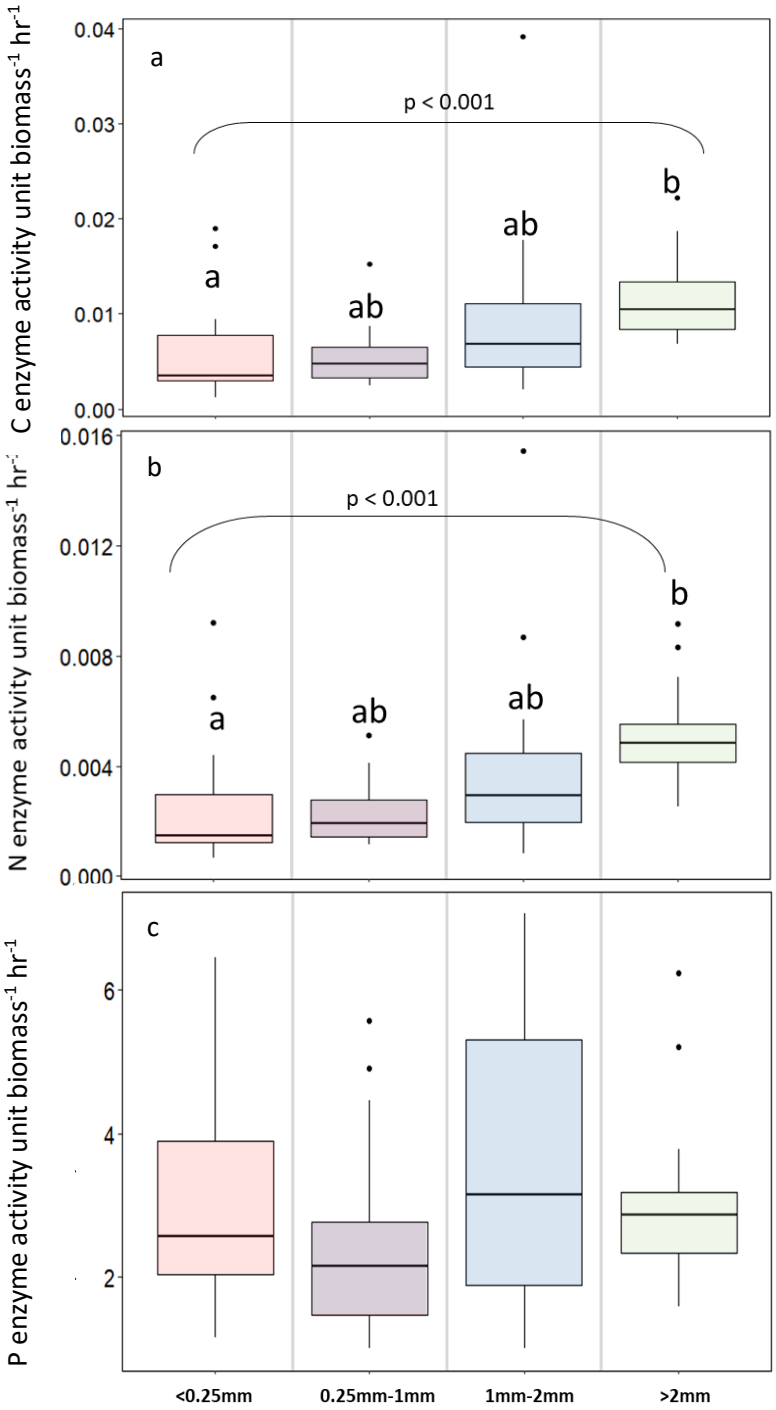

Figure 5: Enzyme activity measured per unit biomass (nmol activity unit biomass^{-1} hr^{-1}). Panel a is the sum of carbon acquiring enzymes (BG + CBH); panel b is total N acquiring enzyme activity (LAP + NAG); panel c is total P acquiring enzyme activity (PHOS). Letters denote significance between aggregate size class. Significance determined by two-way ANOVA.

Carbon use efficiency (CUE) was analyzed to understand microbial investment into growth yield relative to other microbial processes such as stress tolerance mechanisms and nutrient acquisition. Carbon use efficiency varied among aggregate size classes ($F = 3.49$; $p = 0.029$) but was unaffected by tillage ($F = 0.55$; $p > 0.05$) (Figure 6). Mean CUE decreased with increasing aggregate size ranging from 0.27 ± 0.032 in <0.25mm aggregates to 0.17 ± 0.016 in aggregates >2mm.

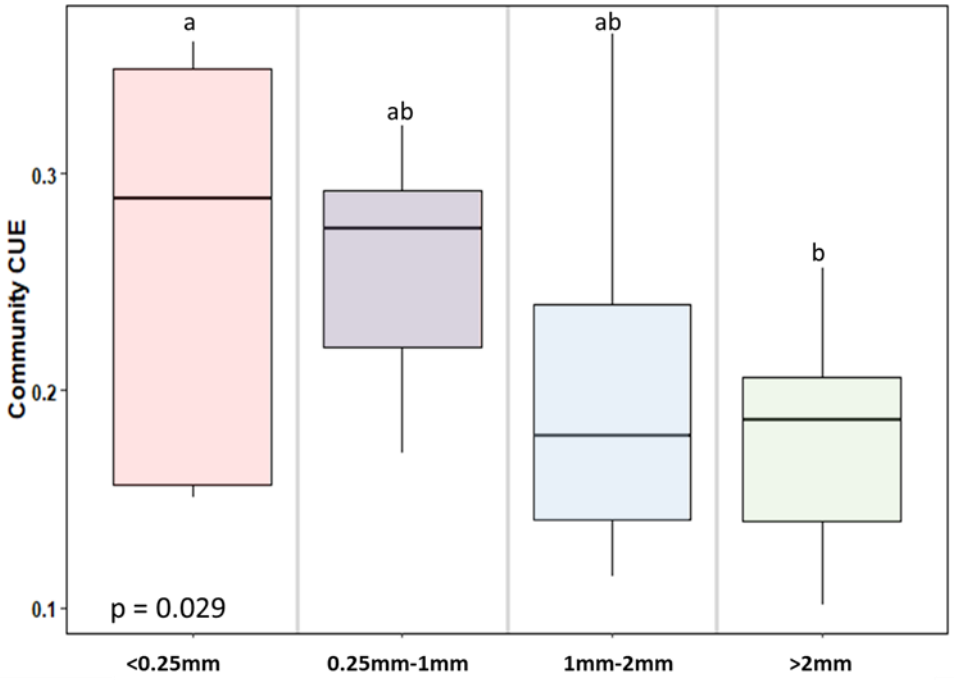

Figure 6: Carbon use efficiency decreased with increasing aggregate size class ($F = 3.49$; $p = 0.029$). Data is averaged across tillage treatment as tillage did not impact CUE ($F = 0.55$; $p > 0.05$). Mean CUE values for aggregate size classes are as follows: <0.25mm 0.27 ± 0.032; 0.25mm-1mm 0.255 ± 0.019; 1mm-2mm 0.20 ± 0.029; >2mm 0.17 ± 0.016

3.5 Predicted Metagenomics

Community weighted mean (CWM) genome size and rRNA copy number were analyzed to confirm measurements of CUE and represent community stress tolerance. Aggregate size class had a significant effect on predicted genome size ($F= 5.029$; $p = 0.004$). In both tillage treatments, CWM genome size in the >2mm aggregate size class was significantly larger than the <0.25mm aggregate size class; averaging 4.54 ± 0.023 and 4.48 ± 0.012 mega base pairs (Mbp) respectively for no-till soils. Under full-till, CWM genome size ranged from 4.46 ± 0.039 to 4.72 ± 0.095 Mbp in <0.25mm and >2mm aggregates respectively. Tillage treatment was nearly significant in the two-way ANOVA model ($p = 0.0802$). CWM rRNA copy number was not affected by either tillage treatment ($F=1.36$; $p > 0.05$) or aggregate size class ($F= 1.81$; $p > 0.05$) (Figure 6b).

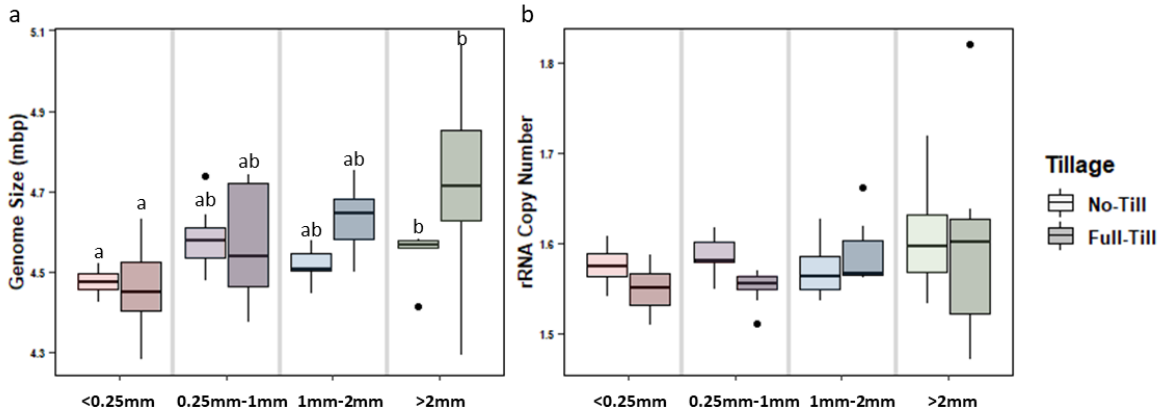

Figure 6: Box plots depicting predicted metagenomic community features. Genome size measured in mega base pairs (a), varied by aggregate size class ($p = 0.004$). Plots are broken out by tillage as tillage was nearly significant in the two-way ANOVA ($p = 0.0802$). Letters denote significance between aggregate sizes in both no-till and full-till treatments. Bars with the same letter are not significantly different ($p < 0.05$). Predicted rRNA gene copy number (b) did not differ by either aggregate size class or tillage treatment.

KEGG orthologs (KO) were predicted via PICRUSt2 (Douglas et al., 2020) which allows for inference into the potential genes, and therefore the potential functions, of the bacterial

community. KO's will hereby be referred to as "predicted genes" or "predicted function". Differential abundance of predicted genes was analyzed to measure traits conferring stress tolerance. All analyses were performed on log transformed, predicted gene abundance. NMDS visualization of PICRUSt predicted genomes shows that community gene composition varies by tillage treatment and aggregate size class (Figure 7). This was confirmed via PERMANOVA (till treatment: $F= 5.41$; $p < 0.001$; aggregate size class: $F= 2.18$; $p < 0.001$). There was also a significant interaction of tillage and aggregate size class on predicted gene composition ($F= 1.68$; $p = 0.003$). To unpack this interaction, PERMANOVA was used to test the effect of tillage on each aggregate size class separately. Aggregates <0.25mm, 1mm-2mm, and >2mm differed in KO abundance with tillage ($p > 0.05$). However, 0.25mm-1mm aggregates were unaffected ($p= 0.116$). The smallest aggregate size classes (<0.25mm and 0.25mm-1mm), points group largely by aggregate size (color) regardless of tillage treatment (shape) (Figure 7b). However, there is a high amount of variability in sample gene composition among larger aggregates (1mm-2mm and >2mm) between tillage treatments indicating that in larger aggregate size classes, agricultural management might be a stronger driver shaping KEGG-predicted function rather than soil structure.

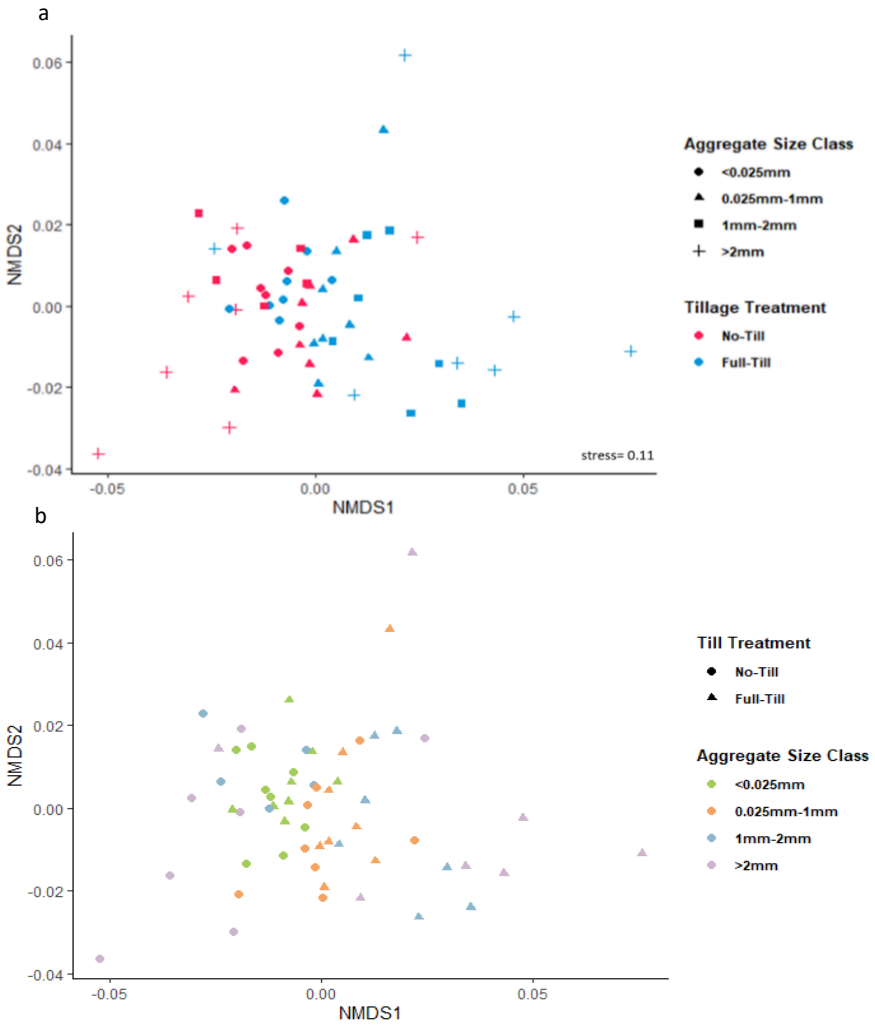

Figure 7: NMDS ordination of community KEGG composition predicted by PICRUSt2. NMDS was performed on log transformed KEGG occurrence using a Bray-Curtis distance matrix. Final stress was 0.11. Both panels (a and b) are the same ordination grouped differently by color. Panel a: points are colored by tillage treatment to highlight the impact of agricultural management on KEGG composition. Panel b: points are colored by aggregate size class to highlight the impact of soil structure on KEGG composition.

Post hoc pairwise comparison of predicted gene composition between aggregate size classes revealed that aggregates <0.25mm differed from 0.25mm- 1mm (Figure 8a; $p < 0.01$), 1mm-2mm (Figure 8b; $p < 0.01$), and >2 mm ($p < 0.05$) aggregate size classes. The top 1% of predicted genes with the highest variance between aggregates were subsampled from an initial pool of 7258 genes. Differential abundance of the 73 high variance genes retained was calculated

between the <0.25mm aggregate size class and all other aggregate sizes (Figure 8). Differences in gene composition between samples were driven largely by the abundance of genes encoding for fatty acid synthesis/metabolism (Figure 8c). Further, stress tolerance genes that encode for cold shock proteins and sigma 70 factors were also enriched in microaggregates (Figure 8c).

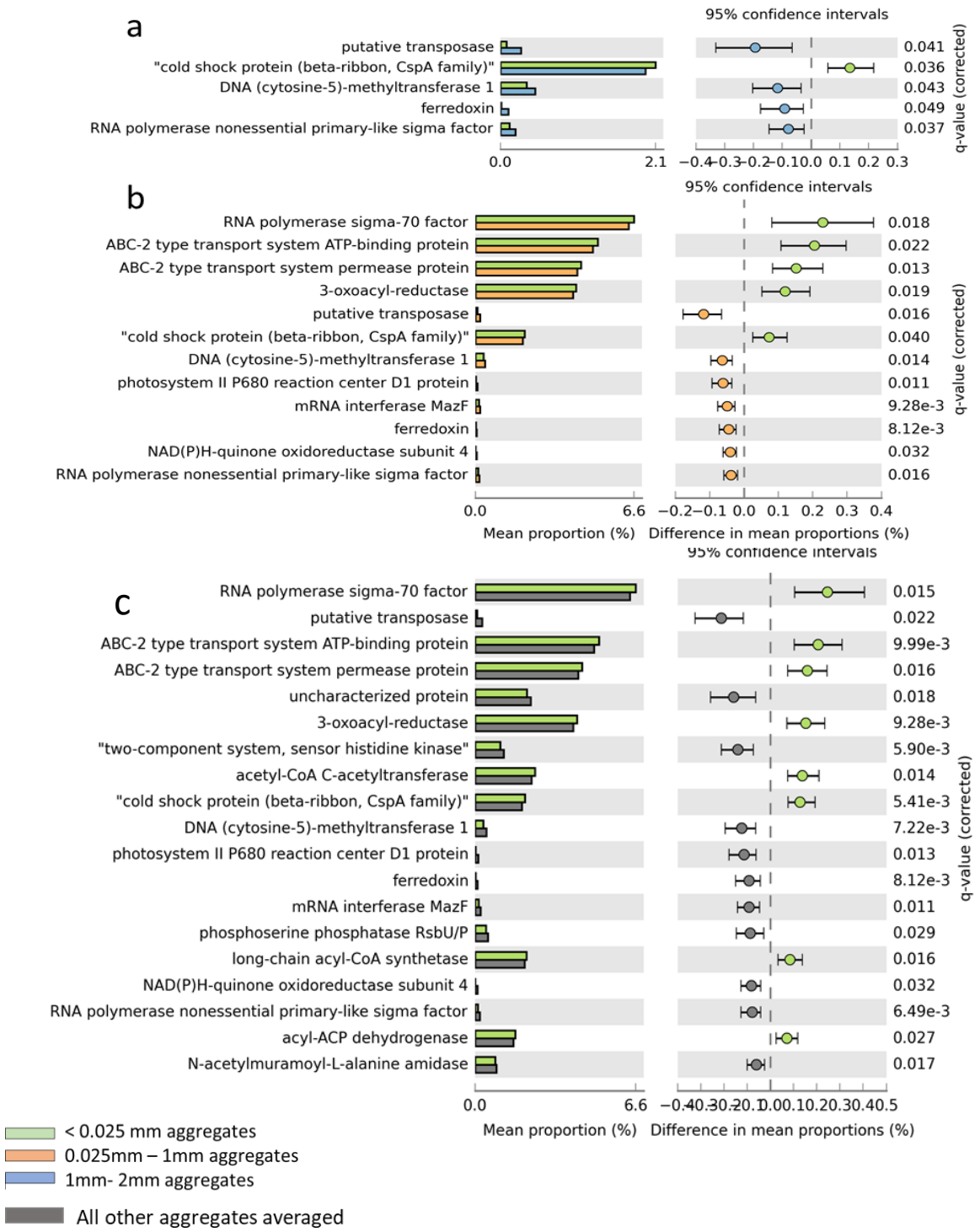

Figure 8: Bacterial functional gene composition analyzed for differential abundance between <0.25mm aggregates and 0.25mm-1mm aggregates (8b), 1mm-2mm aggregates (8a), and across all aggregates averaged (8c). Positive differences in proportions represent greater gene abundance in <0.25mm aggregates (green). Negative differences in proportions represent greater gene abundance in 0.25mm-1mm (orange), 1mm-2mm (blue) and all other aggregates (grey). Corrected P-values were calculated by White's non-parametric t-test with Benjamini-Hochberg FDR correction. False discovery rate (FDR) set at 0.05. q- values represent significance following correction for multiple comparisons. Genes with q-values < 0.05 were considered significant.

3.6 Tradeoffs within the Y-A-S life history framework

Enzyme production and carbon use efficiency were negatively correlated in all aggregate size classes; however, the strength of correlation depended on enzyme type.

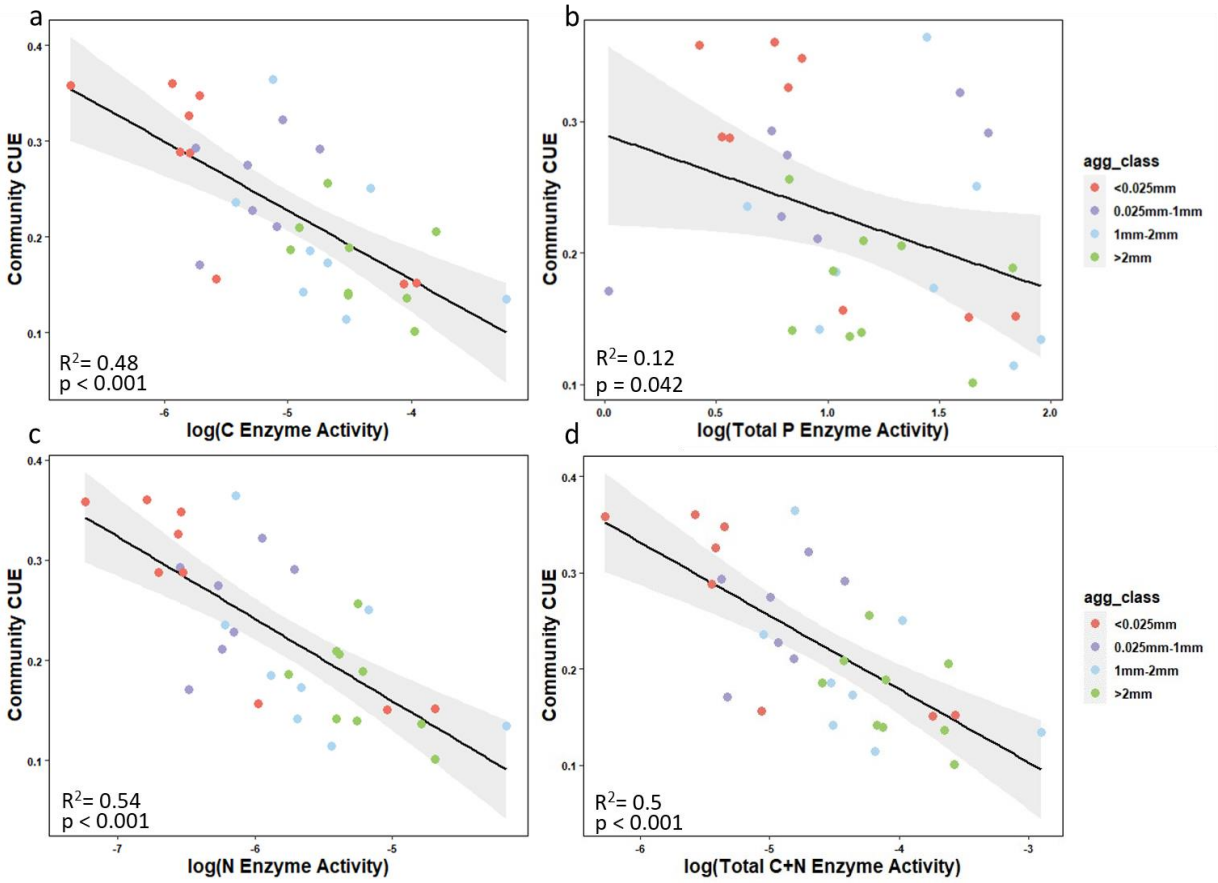

Figure 9: Tradeoffs between log transformed enzyme production and carbon use efficiency across aggregates. All enzyme data was relativized by biomass. Colors represent aggregate size classes. Strength of the regression denoted by R^2.

Linear models determined CUE was negatively correlated with total carbon acquiring, total nitrogen acquiring and total carbon and nitrogen acquiring activity ($p < 0.001$), suggesting that there is a strong tradeoff in microbial investment to growth versus carbon and nitrogen enzyme

acquisition (R^2= 0.50; $p < 0.001$) (Figure 9a, c, d). The relationship between phosphorus acquiring enzymes and carbon use efficiency was less strong however still significant ($p < 0.05$).

4. Discussion

The structural complexity of soils gives rise to innumerable microhabitats including pores of various sizes, intra-aggregate spaces, and the spaces within soil aggregates (Foster, 1988; reviewed by Wilpiszeski et al., 2019). Most studies observe soil microbial function and composition in bulk, by homogenizing the structural complexity of soil. This obscures the complex interplay between microbial communities and the soil physical environments in which they reside (Jilling et al., 2018). For example, habitat variation at the aggregate scale may select for well-adapted microbial species with life history strategies that maximize survival in response to the environmental conditions of the aggregate (Trivedi et al., 2017). At the ecosystem level, understanding the effects of tillage on microbial life history strategies in microhabitats may provide a deeper understanding of the link between agricultural management and carbon storage in soils (Six et al., 2000). The results presented here suggest that observing microbial communities with finer spatial resolution yields insights into the variability of microbial function within soil microhabitats. My findings show that soil aggregates harbor distinct microbial communities with different preferences for specific low molecular weight carbon compounds, and that community carbon use efficiency differs with aggregate size. Additionally, genes conferring stress tolerance vary by aggregate size class. Taken together, these results suggest that tradeoffs within the Y-A-S framework apply to soil aggregate microbial communities and that these relationships persist regardless of tillage

4.1 Abiotic environment and microbial community composition varied by aggregate size class and management

Agricultural management affects both the abiotic and biotic components of soil (Bach et al., 2018; Mbuthia et al., 2015; Schmidt et al., 2018). Relative to no-till soils, tillage changed aggregate size class distribution across my study. Tilled soil had 5.5% more microaggregates and the proportion of aggregates >2mm was significantly reduced compared to no-till soil. While carbon distribution in agricultural soil generally varies depending on both the scale of study (aggregate vs whole field) and agricultural management (Bach et al., 2018; Grandy and Robertson, 2007; Trivedi et al., 2015), bulk soils from the no-till and full-till plots at Kingman Farm do not show differences in total carbon with tillage (Mackay, in preparation) possibly due to the relatively recent adoption of the no-till treatment (7 years). Further, there was no difference in total carbon between aggregate size classes. This may have been a result of the aggregate isolation method chosen, as different methods affect measurements of carbon and nitrogen within aggregates (Xu et al., 2017). Although total carbon did not vary between aggregate size classes, carbon chemistry does generally change with aggregate size (Six et al., 2000). Macroaggregates contain higher levels of dissolved organic carbon and new plant inputs while microaggregates tend to harbor more complex microbially processed forms of carbon (Davinic et al., 2012; Trivedi et al., 2017). These differences in carbon chemistry have been shown to be a stronger driver of community structure than total soil carbon (Davinic et al., 2012). In my study, total nitrogen varied between aggregate size classes; however, this relationship was only seen in no-till treatments.

Both bacterial and fungal community structure were impacted by tillage and aggregate size class. Tillage drives changes in community structure largely due to changes in the chemical

and physical composition of soils (Carbonetto et al., 2014). Community structure in aggregates is driven by both the quality of resources (Davinic et al., 2012) and physical structure of the aggregate environment (Ebrahimi and Or, 2016; Mummey et al., 2006). Pore structure and size within aggregates varies, which might alter microbial access to carbon, driving differences in bacterial community composition between the >2mm and <0.25mm aggregate sizes (Ebrahimi and Or, 2016; Sexstone et al., 1985). In my study, there was no interaction between agricultural management and aggregate size on soil microbial communities suggesting that aggregate communities are being shaped largely by the aggregate environment regardless of management (Bach et al., 2018).

4.2 Microbial physiology varied by aggregate size class

Microbial uptake of labile carbon substrates differed between aggregate size classes however there were no consistent patterns across substrate type. Glucose induced respiration accounted for 25% of total SIR in <0.25mm aggregates. In accordance with a study by Lagomarsino et al. (2012), glucose respiration in this study was inversely related to aggregate size in both full-till and no-till treatments. However, arabinose (also a carbohydrate) elicited an opposite response. Microbial activity in response to citric acid additions accounted for 25% of total SIR in aggregates greater than 1mm and increased with increasing aggregate size contrasting the findings of Lagomarsino et al. (2012). Organic acids (such as citric and malic acid) constitute a large proportion of plant root exudates (Tawaraya et al., 2014). Exudates are effused by plant roots to attract beneficial microbes to the rhizosphere and to mine for nutrients (Tawaraya et al., 2014). Given the role of plant roots as binding agents in macroaggregate formation (Tisdall and Oades, 1982), microbial communities in larger aggregates may be more adept at utilizing organic acids. Interestingly, although patterns of substrate utilization differed

among type of compound (carbohydrate/ organic acid), there were no differences in total SIR among aggregate size classes.

Microbes must satisfy their nutrient and resource demand through either the direct uptake of simple compounds or through investment into enzymes (Mooshammer et al., 2014). This investment of resources into enzyme production comes with a tradeoff, so enzyme activity was measured to infer microbial investment into resource acquisition relative to investment in yield or stress tolerance. Individual carbon acquiring enzymes (BG and CBH) were unaffected by aggregate size. CBH however, was significantly lower in full-tilled treatments which could be a result of changes in fungal community composition due to soil disturbance (Helgason et al., 2010; Kyaschenko et al., 2017). When total carbon and total nitrogen acquiring enzymes were studied, patterns emerged with aggregate size. Investment into both total nitrogen and total carbon acquiring enzymes were higher in >2mm aggregates relative to <0.25mm and 0.25mm-1mm aggregates suggesting that macroaggregate communities may harbor acquisition strategists. High enzyme production in macroaggregates could be a result of favorable pore structure and diffusion gradients. Enzymes produced exogenously diffuse into the environment to reach their target substrate thus resource acquisition via enzyme production should be favored in environments with high pore connectivity such as macroaggregates (Rabbi et al., 2016). Despite often having more complex carbon in need of enzymatic depolymerization, microaggregates may be unfavorable environments for diffusion due to low porosity making return on investment into enzymes low (Rabbi, 2016).

Substrate- independent carbon use efficiency methods capture measures of *in situ* efficiency due to the constraints imposed by the environment (Geyer et al., 2019). Thus, this method represents microbial strategies (e.g. yield) in response to the aggregate environment. The

values reported in this study fall within the same range of other studies using substrate nonspecific carbon use efficiency (Geyer et al., 2019; Malik et al., 2019). Contrary to my hypotheses, carbon use efficiency declined with increasing aggregate size class and this relationship was not impacted by agricultural management. Although not what was predicted, high yield may be advantageous to organisms in microaggregates where carbon resources are scarce and often physically occluded. CUE has been shown to decline with increasing aggregate size previously (Liu et al., 2021), however microhabitat variation in carbon use efficiency is understudied (Anthony et al., 2020).

4.3 Predicted metagenomic features differ by aggregate size class

Agricultural management, and resultant changes in abiotic soil properties, impact the genomic potential of soil microorganisms (Trivedi et al., 2015). In accordance with my hypothesis, predicted metagenomic features differed between aggregate size classes and this relationship was modulated by agricultural management. Specifically, community weighted mean genome size increased significantly with increasing aggregate size. This relationship may be the result of differences in the stability of aggregates as microbial habitats. Microaggregates are more stable environments with slower turnover times and longer persistence (Al-Kaisi et al., 2014), and larger genomes are favored in variable environments while stable environments select for smaller genomes (Bentkowski et al., 2015). Thus, differences in stability between macroaggregates and microaggregates may impose selection pressure that drives genome size. Further supporting this idea, the relationship between genome size and aggregate size was exacerbated by agricultural management. In both no-till and full-till treatments, aggregates <0.25mm had similar genome sizes (4.48 ± 0.012 and 4.46 ± 0.039 mega base pairs respectively). However, genome size in aggregates >2mm diverged between no-till and full-till

soils (4.54 ± 0.023 and 4.72 ± 0.095 mega base pairs respectively). Tillage decreases macroaggregate stability (Al-Kaisi et al., 2014) which makes the potential relationship between genome size and habitat stability even more apparent within macroaggregates. rRNA gene copy number is a genomic feature included in most studies of bacterial life history strategy (Fierer et al., 2007; Krause et al., 2014; Schmidt et al., 2018) as it is correlated with bacterial growth rate (Klappenbach et al., 2000; Roller et al., 2016). However unlike other life history frameworks, within the Y-A-S framework, growth rate is an emergent property of the microbial community and not a strategy in and of its self (Malik et al., 2020a). Therefore, it was unsurprising that there was no correlation between rRNA gene copy number and the metrics studied here.

The frequency of functional genes within a community is also important for determining microbial functional capabilities and life history strategy (Wood et al., 2018). Gene composition of aggregates <0.25mm differed from both the 0.25mm-1mm and 1mm-2mm aggregate size classes. Analyzing microaggregates against all other aggregates revealed genes driving functional differences. Of the 8 genes significantly enriched in <0.25mm aggregate size class, 4 of these genes were related to fatty acid synthesis or metabolism: long-chain acyl-CoA synthetase (Black et al., 2000), acyl-ACP dehydrogenase (Yao and Rock, 2017), 3-oxoacyl-reductase (Guo et al., 2019), and acetyl-coa c-acetyltransferase. Genetic markers related to cell wall biosynthesis are hypothesized to confer stress tolerance due to their role in maintaining cellular integrity. Stress tolerance is largely conferred by cell membrane chemistry given that this is the only barrier of defense between a cell and the surrounding environment (Russell et al., 1995). Genes encoding for cold shock proteins (Csp) were also enriched in aggregates <0.25mm. Despite their name, many families of Csp genes are also important in microbial response to osmotic, oxidative, and starvation stress (reviewed by Keto-Timonen et al., 2016). Thus, their

enrichment in aggregates <0.25 mm further supports the notion that microaggregates harbor a stress tolerant community. Sigma factors are RNA polymerase subunits responsible for transcription initiation (Paget, 2015). Sigma 70 contains four subgroups of sigma factors, 3 of which are involved in response to nutrient limitation, oxidative and osmotic stress (Paget, 2015). Predicted genes coding for RNA polymerase sigma 70 factors were significantly enriched in microaggregates which provides evidence of stress tolerance (Malik et al., 2020).

4.4 Tradeoffs exist between growth Yield and Acquisition regardless of management. Microaggregates harbor stress tolerant communities

Studying physiological and metagenomic characteristics of aggregate microbial communities has revealed potential life history strategies that vary by aggregate size. In accordance with my hypothesis, predictive genomic features point to microbial communities within microaggregates as Stress tolerator communities regardless of tillage. Community weighted mean genome sizes were significantly smaller in aggregates <0.25mm. This may confer stress tolerance because streamlined genomes may be advantageous in resource-poor environments due to fewer resources needed to maintain and reproduce smaller genomes (Giovannoni et al., 2014). Additionally, six of eight predicted genes enriched in microaggregate communities were potentially related to stress tolerance. The remaining two genes were related to ABC membrane transporters responsible for uptake of simple molecules which could put microaggregates in the hypothesized 4th corner (stress/resource limited) section of the Y-A-S framework (Malik et al., 2019). It must be noted that most of these genes and related functions have been explored in single organism, culture-based studies (mainly of *E.* coli) and their role in stress tolerance in mixed soil communities has yet to be tested.

The ultimate goal of the Y-A-S framework is to predict microbially driven ecosystem function and response to environmental change by simplifying the vast genetic diversity in soils into meaningful functional groups. Microbial function often cannot be predicted by genes alone (Pold et al., 2020), therefore it is important to turn to physiological measurements that reflect *in situ* tradeoffs in resources. CUE was negatively correlated with enzyme production for both carbon and nitrogen acquiring enzymes. This tradeoff between yield and investment into resource acquisition is consistent with the Y-A-S framework (Malik et al., 2020, 2019). However, the tradeoff between CUE and phosphorus acquiring enzymes was less apparent. There were no discernable patterns of acquisition related to simple carbon molecules within aggregate sizes. This lack of relationship between CUE and multiple SIR may suggest the genomic machinery for carbon uptake does not come at an overall cost to Yield. It should be noted that enzyme activity and carbon use efficiency measurements represent one time point and thus further research should be conducted to assess these relationships over time and across fluctuating environmental conditions.

Although there were apparent tradeoffs between Yield and Acquisition strategies, the tradeoffs with Stress tolerant strategies deserve further study. There was a negative relationship between genome size and CUE ($R^2 = 0.28$; $p = 0.003$) providing putative support for tradeoffs with stress tolerance however, more work needs to be done to confirm the benefits of streamlined genomes. Microaggregate communities had high CUE and an abundance of genes conferring stress tolerance which may suggest that Stress tolerator communities do not have inherently lower yield or that the Y-S tradeoff may exist only when presented with unfavorable abiotic conditions. CUE is a dynamic trait dependent on both genomic constraints on physiology and the conditions of the surrounding environment (Domeignoz-Horta et al., 2020). Therefore, further

work needs to be done to verify the S-A and S-Y tradeoffs in microaggregates with varying levels of abiotic stress.

Microbial life history strategies determine the fate of carbon which could have large implications for maintaining healthy agricultural systems. As shown in this study, tillage shifts the distribution of aggregates thus changing the proportions of microbes classified by Yield, Acquisition and Stress tolerance. Understanding the environmental scale and functional outcomes associated with microbial community life histories may allow us to better predict how ecosystem function will shift in response to soil management activities.

5. References

Al-Kaisi, M.M., Douelle, A., Kwaw-Mensah, D., 2014. Soil microaggregate and macroaggregate decay over time and soil carbon change as influenced by different tillage systems. Journal of Soil and Water Conservation 69, 574–580. doi:10.2489/jswc.69.6.574

Allison, S.D., Goulden, M.L., 2017. Consequences of drought tolerance traits for microbial decomposition in the DEMENT model. Soil Biology and Biochemistry 107, 104–113. doi:10.1016/j.soilbio.2017.01.001

Anderson, J.P.E., Domsch, K.H., 1978. A physiological method for the quantitative measurement of microbial biomass in soils. Soil Biology and Biochemistry 10, 215–221. doi:10.1016/0038-0717(78)90099-8

Anthony, M.A., Crowther, T.W., Maynard, D.S., van den Hoogen, J., Averill, C., 2020. Distinct Assembly Processes and Microbial Communities Constrain Soil Organic Carbon Formation. One Earth 2, 349–360. doi:10.1016/j.oneear.2020.03.006

Bach, E.M., Hofmockel, K.S., 2014. Soil aggregate isolation method affects measures of intra-aggregate extracellular enzyme activity. Soil Biology and Biochemistry 69, 54–62. doi:10.1016/j.soilbio.2013.10.033

Bach, E.M., Williams, R.J., Hargreaves, S.K., Yang, F., Hofmockel, K.S., 2018. Greatest soil microbial diversity found in micro-habitats. Soil Biology and Biochemistry 118, 217–226. doi:10.1016/j.soilbio.2017.12.018

Bailey, V.L., McCue, L.A., Fansler, S.J., Boyanov, M.I., DeCarlo, F., Kemner, K.M., Konopka, A., 2013. Micrometer-scale physical structure and microbial composition of soil macroaggregates. Soil Biology and Biochemistry 65, 60–68. doi:10.1016/j.soilbio.2013.02.005

Bentkowski, P., Van Oosterhout, C., Mock, T., 2015. A Model of Genome Size Evolution for Prokaryotes in Stable and Fluctuating Environments. Genome Biology and Evolution 7, 2344–2351. doi:10.1093/gbe/evv148

Black, P.N., Færgeman, N.J., DiRusso, C.C., 2000. Long-Chain Acyl-CoA–Dependent Regulation of Gene Expression in Bacteria, Yeast and Mammals. The Journal of Nutrition 130, 305S-309S. doi:10.1093/jn/130.2.305S

Bolyen, E., Rideout, J.R., Dillon, M.R., Bokulich, N.A., Abnet, C.C., Al-Ghalith, G.A., Alexander, H., Alm, E.J., Arumugam, M., Asnicar, F., Bai, Y., Bisanz, J.E., Bittinger, K., Brejnrod, A., Brislawn, C.J., Brown, C.T., Callahan, B.J., Caraballo-Rodríguez, A.M., Chase, J., Cope, E.K., Da Silva, R., Diener, C., Dorrestein, P.C., Douglas, G.M., Durall, D.M., Duvallet, C., Edwardson, C.F., Ernst, M., Estaki, M., Fouquier, J., Gauglitz, J.M., Gibbons, S.M., Gibson, D.L., Gonzalez, A., Gorlick, K., Guo, J., Hillmann, B., Holmes, S., Holste, H., Huttenhower, C., Huttley, G.A., Janssen, S., Jarmusch, A.K., Jiang, L., Kaehler, B.D., Kang, K.B., Keefe, C.R., Keim, P., Kelley, S.T., Knights, D., Koester, I., Kosciolek, T., Kreps, J., Langille, M.G.I., Lee, J., Ley, R., Liu, Y.-X., Loftfield, E., Lozupone, C., Maher, M., Marotz, C., Martin, B.D., McDonald, D., McIver, L.J., Melnik, A.V., Metcalf, J.L., Morgan, S.C., Morton, J.T., Naimey, A.T., Navas-Molina, J.A., Nothias, L.F., Orchanian, S.B., Pearson, T., Peoples, S.L., Petras, D., Preuss, M.L., Pruesse, E., Rasmussen, L.B., Rivers, A., Robeson, M.S., Rosenthal, P., Segata, N., Shaffer, M., Shiffer, A., Sinha, R., Song, S.J., Spear, J.R., Swafford, A.D., Thompson, L.R., Torres, P.J., Trinh, P., Tripathi, A., Turnbaugh, P.J., Ul-Hasan, S., van der Hooft, J.J.J., Vargas, F., Vázquez-Baeza, Y., Vogtmann, E., von Hippel, M., Walters, W., Wan, Y., Wang, M., Warren, J., Weber, K.C., Williamson, C.H.D., Willis, A.D., Xu, Z.Z., Zaneveld, J.R., Zhang, Y., Zhu, Q., Knight, R., Caporaso, J.G., 2019. Reproducible, interactive, scalable and extensible microbiome data science using QIIME 2. Nature Biotechnology 37, 852–857. doi:10.1038/s41587-019-0209-9

Callahan, B.J., McMurdie, P.J., Rosen, M.J., Han, A.W., Johnson, A.J.A., Holmes, S.P., 2016. DADA2: High-resolution sample inference from Illumina amplicon data. Nature Methods 13, 581–583. doi:10.1038/nmeth.3869

Campbell, C.D., Chapman, S.J., Cameron, C.M., Davidson, M.S., Potts, J.M., 2003. A Rapid Microtiter Plate Method To Measure Carbon Dioxide Evolved from Carbon Substrate Amendments so as To Determine the Physiological Profiles of Soil Microbial Communities by Using Whole Soil. Applied and Environmental Microbiology 69, 3593–3599. doi:10.1128/AEM.69.6.3593-3599.2003

Carbonetto, B., Rascovan, N., Alvarez, R., Mentaberry, A., Vazquez, M.P., 2014. Structure, Composition and Metagenomic Profile of Soil Microbiomes Associated to Agricultural Land Use and Tillage Systems in Argentine Pampas. Plos One 9, e99949. doi:10.1371/journal.pone.0099949

Davinic, M., Fultz, L.M., Acosta-Martinez, V., Calderón, F.J., Cox, S.B., Dowd, S.E., Allen, V.G., Zak, J.C., Moore-Kucera, J., 2012. Pyrosequencing and mid-infrared spectroscopy reveal distinct aggregate stratification of soil bacterial communities and organic matter composition. Soil Biology and Biochemistry 46, 63–72. doi:10.1016/j.soilbio.2011.11.012

Domeignoz-Horta, L.A., Pold, G., Liu, X.-J.A., Frey, S.D., Melillo, J.M., DeAngelis, K.M., 2020. Microbial diversity drives carbon use efficiency in a model soil. Nature Communications 11, 3684. doi:10.1038/s41467-020-17502-z

Douglas, G.M., Maffei, V.J., Zaneveld, J., Yurgel, S.N., Brown, J.R., Taylor, C.M., Huttenhower, C., Langille, M.G.I., n.d. PICRUSt2: An improved and extensible approach for metagenome inference 42.

Ebrahimi, A., Or, D., 2016. Hydration and diffusion processes shape microbial community organization and function in model soil aggregates. Water Resources Research 24.

Fierer, N., Bradford, M.A., Jackson, R.B., 2007. Toward an Ecological Classification of Soil Bacteria. Ecology 88, 1354–1364. doi:10.1890/05-1839

Foster, R.C., 1988. Microenvironments of soil microorganisms. Biology and Fertility of Soils 6. doi:10.1007/BF00260816

German, D.P., Weintraub, M.N., Grandy, A.S., Lauber, C.L., Rinkes, Z.L., Allison, S.D., 2011. Optimization of hydrolytic and oxidative enzyme methods for ecosystem studies. Soil Biology and Biochemistry 43, 1387–1397. doi:10.1016/j.soilbio.2011.03.017

Geyer, K.M., Dijkstra, P., Sinsabaugh, R., Frey, S.D., 2019. Clarifying the interpretation of carbon use efficiency in soil through methods comparison. Soil Biology and Biochemistry 128, 79–88. doi:10.1016/j.soilbio.2018.09.036

Giovannoni, S.J., Cameron Thrash, J., Temperton, B., 2014. Implications of streamlining theory for microbial ecology. The ISME Journal 8, 1553–1565. doi:10.1038/ismej.2014.60

Grandy, A.S., Robertson, G.P., 2007. Land-Use Intensity Effects on Soil Organic Carbon Accumulation Rates and Mechanisms. Ecosystems 10, 59–74. doi:10.1007/s10021-006-9010-y

Gravuer, K., Eskelinen, A., 2017. Nutrient and Rainfall Additions Shift Phylogenetically Estimated Traits of Soil Microbial Communities. Frontiers in Microbiology 8, 1271. doi:10.3389/fmicb.2017.01271

Grime, J.P., 1977. Evidence for the Existence of Three Primary Strategies in Plants and Its Relevance to Ecological and Evolutionary Theory. The American Naturalist 111, 1169–1194.

Guan, N., Liu, L., 2020. Microbial response to acid stress: mechanisms and applications. Applied Microbiology and Biotechnology 104, 51–65. doi:10.1007/s00253-019-10226-1

Guo, Q.-Q., Zhang, W.-B., Zhang, C., Song, Y.-L., Liao, Y.-L., Ma, J.-C., Yu, Y.-H., Wang, H.-H., 2019. Characterization of 3-Oxacyl-Acyl Carrier Protein Reductase Homolog Genes in Pseudomonas aeruginosa PAO1. Frontiers in Microbiology 10, 1028. doi:10.3389/fmicb.2019.01028

Helgason, B.L., Walley, F.L., Germida, J.J., 2010. No-till soil management increases microbial biomass and alters community profiles in soil aggregates. Applied Soil Ecology 46, 390–397. doi:10.1016/j.apsoil.2010.10.002

Jilling, A., Keiluweit, M., Contosta, A.R., Frey, S., Schimel, J., Schnecker, J., Smith, R.G., Tiemann, L., Grandy, A.S., 2018. Minerals in the rhizosphere: overlooked mediators of soil nitrogen availability to plants and microbes. Biogeochemistry 139, 103–122. doi:10.1007/s10533-018-0459-5

Kallenbach, C.M., Frey, S.D., Grandy, A.S., 2016. Direct evidence for microbial-derived soil organic matter formation and its ecophysiological controls. Nature Communications 7, 13630. doi:10.1038/ncomms13630

Kallenbach, C.M., Grandy, A.S., Frey, S.D., Diefendorf, A.F., 2015. Microbial physiology and necromass regulate agricultural soil carbon accumulation. Soil Biology and Biochemistry 91, 279–290. doi:10.1016/j.soilbio.2015.09.005

Kembel, S.W., Cowan, P.D., Helmus, M.R., Cornwell, W.K., Morlon, H., Ackerly, D.D., Blomberg, S.P., Webb, C.O., 2010. Picante: R tools for integrating phylogenies and ecology. Bioinformatics 26, 1463–1464. doi:10.1093/bioinformatics/btq166

Kembel, S.W., Wu, M., Eisen, J.A., Green, J.L., 2012. Incorporating 16S Gene Copy Number Information Improves Estimates of Microbial Diversity and Abundance. PLoS Computational Biology 8. doi:10.1371/journal.pcbi.1002743

Keto-Timonen, R., Hietala, N., Palonen, E., Hakakorpi, A., Lindström, M., Korkeala, H., 2016. Cold Shock Proteins: A Minireview with Special Emphasis on Csp-family of Enteropathogenic Yersinia. Frontiers in Microbiology 7. doi:10.3389/fmicb.2016.01151

Klappenbach, J.A., Dunbar, J.M., Schmidt, T.M., 2000. rRNA Operon Copy Number Reflects Ecological Strategies of Bacteria. Applied and Environmental Microbiology 66, 1328–1333. doi:10.1128/AEM.66.4.1328-1333.2000

Krause, S., Le Roux, X., Niklaus, P.A., Van Bodegom, P.M., Lennon, J.T., Bertilsson, S., Grossart, H.-P., Philippot, L., Bodelier, P.L.E., 2014. Trait-based approaches for understanding microbial biodiversity and ecosystem functioning. Frontiers in Microbiology 5. doi:10.3389/fmicb.2014.00251

Kyaschenko, J., Clemmensen, K.E., Hagenbo, A., Karltun, E., Lindahl, B.D., 2017. Shift in fungal communities and associated enzyme activities along an age gradient of managed Pinus sylvestris stands. The ISME Journal 11, 863–874. doi:10.1038/ismej.2016.184

Lal, R., 2010. Enhancing Eco-efficiency in Agro-ecosystems through Soil Carbon Sequestration. Crop Science 50, S-120-S-131. doi:10.2135/cropsci2010.01.0012

Liu, X.J.A., Pold, G., Domeignoz-Horta, L.A., Geyer, K.M., Caris, H., Nicolson, H., Kemner, K.M., Frey, S.D., Melillo, J.M., DeAngelis, K.M., 2021. Soil aggregate-mediated microbial responses to long-term warming. Soil Biology and Biochemistry 152, 108055. doi:10.1016/j.soilbio.2020.108055

Louca, S., Doebeli, M., 2018. Efficient comparative phylogenetics on large trees. Bioinformatics 34, 1053–1055. doi:10.1093/bioinformatics/btx701

Malik, A.A., Martiny, J.B.H., Brodie, E.L., Martiny, A.C., Treseder, K.K., Allison, S.D., 2020a. Defining trait-based microbial strategies with consequences for soil carbon cycling under climate change. The ISME Journal 1–9. doi:10.1038/s41396-019-0510-0

Malik, A.A., Martiny, J.B.H., Brodie, E.L., Martiny, A.C., Treseder, K.K., Allison, S.D., 2020b. Defining trait-based microbial strategies with consequences for soil carbon cycling under climate change. The ISME Journal 14, 1–9. doi:10.1038/s41396-019-0510-0

Malik, A.A., Puissant, J., Goodall, T., Allison, S.D., Griffiths, R.I., 2019. Soil microbial communities with greater investment in resource acquisition have lower growth yield. Soil Biology and Biochemistry 132, 36–39. doi:10.1016/j.soilbio.2019.01.025

Matsen, F.A., Kodner, R.B., Armbrust, E.V., 2010. pplacer: linear time maximum-likelihood and Bayesian phylogenetic placement of sequences onto a fixed reference tree. BMC Bioinformatics 11, 538. doi:10.1186/1471-2105-11-538

Mbuthia, L.W., Acosta-Martínez, V., DeBruyn, J., Schaeffer, S., Tyler, D., Odoi, E., Mpheshea, M., Walker, F., Eash, N., 2015. Long term tillage, cover crop, and fertilization effects on microbial community structure, activity: Implications for soil quality. Soil Biology and Biochemistry 89, 24–34. doi:10.1016/j.soilbio.2015.06.016

Moscatelli, M.C., Secondi, L., Marabottini, R., Papp, R., Stazi, S.R., Mania, E., Marinari, S., 2018. Assessment of soil microbial functional diversity: land use and soil properties affect CLPP-MicroResp and enzymes responses. Pedobiologia 66, 36–42. doi:10.1016/j.pedobi.2018.01.001

Mummey, D., Holben, W., Six, J., Stahl, P., 2006. Spatial Stratification of Soil Bacterial Populations in Aggregates of Diverse Soils 8.

Nilsson, R.H., Larsson, K.-H., Taylor, A.F.S., Bengtsson-Palme, J., Jeppesen, T.S., Schigel, D., Kennedy, P., Picard, K., Glöckner, F.O., Tedersoo, L., Saar, I., Kõljalg, U., Abarenkov, K., 2019. The UNITE database for molecular identification of fungi: handling dark taxa and parallel taxonomic classifications. Nucleic Acids Research 47, D259–D264. doi:10.1093/nar/gky1022

Paget, M., 2015. Bacterial Sigma Factors and Anti-Sigma Factors: Structure, Function and Distribution. Biomolecules 5, 1245–1265. doi:10.3390/biom5031245

Parks, D.H., Tyson, G.W., Hugenholtz, P., Beiko, R.G., 2014. STAMP: statistical analysis of taxonomic and functional profiles. Bioinformatics 30, 3123–3124. doi:10.1093/bioinformatics/btu494

Pold, G., Domeignoz-Horta, L.A., Morrison, E.W., Frey, S.D., Sistla, S.A., DeAngelis, K.M., 2020. Carbon Use Efficiency and Its Temperature Sensitivity Covary in Soil Bacteria. MBio 11, e02293-19, /mbio/11/1/mBio.02293-19.atom. doi:10.1128/mBio.02293-19

Prommer, J., Walker, T.W.N., Wanek, W., Braun, J., Zezula, D., Hu, Y., Hofhansl, F., Richter, A., 2020. Increased microbial growth, biomass, and turnover drive soil organic carbon accumulation at higher plant diversity. Global Change Biology 26, 669–681. doi:10.1111/gcb.14777

Rabbi, S.M.F., 2016. Physical soil architectural traits are functionally linked to carbon decomposition and bacterial diversity. Scientific Reports 9.

Ramin, K.I., Allison, S.D., 2019. Bacterial Tradeoffs in Growth Rate and Extracellular Enzymes. Frontiers in Microbiology 10, 2956. doi:10.3389/fmicb.2019.02956

Rivers, A.R., Weber, K.C., Gardner, T.G., Liu, S., Armstrong, S.D., 2018. ITSxpress: Software to rapidly trim internally transcribed spacer sequences with quality scores for marker gene analysis. F1000Research 7, 1418. doi:10.12688/f1000research.15704.1

Roller, B.R.K., Stoddard, S.F., Schmidt, T.M., 2016. Exploiting rRNA Operon Copy Number to Investigate Bacterial Reproductive Strategies. Nature Microbiology 1, 16160. doi:10.1038/nmicrobiol.2016.160

Russell, N.J., Evans, R.I., ter Steeg, P.F., Hellemons, J., Verheul, A., Abee, T., 1995. Membranes as a target for stress adaptation. International Journal of Food Microbiology 28, 255–261. doi:10.1016/0168-1605(95)00061-5

Saiya-Cork, K.R., Sinsabaugh, R.L., Zak, D.R., 2002. The effects of long term nitrogen deposition on extracellular enzyme activity in an Acer saccharum forest soil. Soil Biology and Biochemistry 34, 1309–1315. doi:10.1016/S0038-0717(02)00074-3

Schimel, J., Balser, T.C., Wallenstein, M., 2007. MICROBIAL STRESS-RESPONSE PHYSIOLOGY AND ITS IMPLICATIONS FOR ECOSYSTEM FUNCTION. Ecology 88, 1386–1394. doi:10.1890/06-0219

Schmidt, R., Gravuer, K., Bossange, A.V., Mitchell, J., Scow, K., 2018. Long-term use of cover crops and no-till shift soil microbial community life strategies in agricultural soil. PLOS ONE 13, e0192953. doi:10.1371/journal.pone.0192953

Sexstone, A.J., Revsbech, N.P., Parkin, T.B., Tiedje, J.M., 1985. Direct Measurement of Oxygen Profiles and Denitrification Rates in Soil Aggregates. Soil Science Society of America Journal 49, 645–651. doi:10.2136/sssaj1985.03615995004900030024x

Six, J., Paustian, K., Elliott, E.T., Combrink, C., 2000. Soil Structure and Organic Matter I. Distribution of Aggregate-Size Classes and Aggregate-Associated Carbon. Soil Science Society of America Journal 64, 681–689. doi:10.2136/sssaj2000.642681x

Spohn, M., Klaus, K., Wanek, W., Richter, A., 2016. Microbial carbon use efficiency and biomass turnover times depending on soil depth – Implications for carbon cycling. Soil Biology and Biochemistry 96, 74–81. doi:10.1016/j.soilbio.2016.01.016

Tawaraya, K., Horie, R., Shinano, T., Wagatsuma, T., Saito, K., Oikawa, A., 2014. Metabolite profiling of soybean root exudates under phosphorus deficiency. Soil Science and Plant Nutrition 60, 679–694. doi:10.1080/00380768.2014.945390

Tiemann, L.K., Grandy, A.S., Atkinson, E.E., Marin-Spiotta, E., McDaniel, M.D., 2015. Crop rotational diversity enhances belowground communities and functions in an agroecosystem. Ecology Letters 18, 761–771. doi:10.1111/ele.12453

Tisdall, J.M., Oades, J.M., 1982. Organic matter and water-stable aggregates in soils. Journal of Soil Science 33, 141–163. doi:10.1111/j.1365-2389.1982.tb01755.x

Trivedi, P., Delgado-Baquerizo, M., Jeffries, T.C., Trivedi, C., Anderson, I.C., Lai, K., McNee, M., Flower, K., Singh, B.P., Minkey, D., Singh, B.K., 2017a. Soil aggregation and associated microbial communities modify the impact of agricultural management on carbon content. Environmental Microbiology 19, 3070–3086. doi:10.1111/1462-2920.13779

Trivedi, P., Delgado-Baquerizo, M., Jeffries, T.C., Trivedi, C., Anderson, I.C., Lai, K., McNee, M., Flower, K., Singh, B.P., Minkey, D., Singh, B.K., 2017b. Soil aggregation and associated microbial communities modify the impact of agricultural management on carbon content. Environmental Microbiology 19, 3070–3086. doi:10.1111/1462-2920.13779

Trivedi, P., Rochester, I.J., Trivedi, C., Van Nostrand, J.D., Zhou, J., Karunaratne, S., Anderson, I.C., Singh, B.K., 2015. Soil aggregate size mediates the impacts of cropping regimes on soil carbon and microbial communities. Soil Biology and Biochemistry 91, 169–181. doi:10.1016/j.soilbio.2015.08.034

Wallenstein, M.D., Hall, E.K., 2012. A trait-based framework for predicting when and where microbial adaptation to climate change will affect ecosystem functioning. Biogeochemistry 109, 35–47. doi:10.1007/s10533-011-9641-8

Walters, W., Hyde, E.R., Berg-Lyons, D., Ackermann, G., Humphrey, G., Parada, A., Gilbert, J.A., Jansson, J.K., Caporaso, J.G., Fuhrman, J.A., Apprill, A., Knight, R., 2016. Improved Bacterial 16S rRNA Gene (V4 and V4-5) and Fungal Internal Transcribed Spacer Marker Gene Primers for Microbial Community Surveys. MSystems 1, sys0029, e00009-15. doi:10.1128/mSystems.00009-15

Wanek, W., 2014. Stoichiometric imbalances between terrestrial decomposer communities and their resources: mechanisms and implications of microbial adaptations to their resources. Frontiers in Microbiology 10.

Wieder, W.R., Bonan, G.B., Allison, S.D., 2013. Global soil carbon projections are improved by modelling microbial processes. Nature Climate Change 3, 909–912. doi:10.1038/nclimate1951

Wieder, W.R., Grandy, A.S., Kallenbach, C.M., Taylor, P.G., Bonan, G.B., 2015. Representing life in the Earth system with soil microbial functional traits in the MIMICS model. Geoscientific Model Development Discussions 8, 2011–2052. doi:10.5194/gmdd-8-2011-2015

Wilpiszeski, R.L., Aufrecht, J.A., Retterer, S.T., Sullivan, M.B., Graham, D.E., Pierce, E.M., Zablocki, O.D., Palumbo, A.V., Elias, D.A., 2019a. Soil Aggregate Microbial Communities: Towards Understanding Microbiome Interactions at Biologically Relevant Scales. Applied and Environmental Microbiology 85, e00324-19, /aem/85/14/AEM.00324-19.atom. doi:10.1128/AEM.00324-19

Wilpiszeski, R.L., Aufrecht, J.A., Retterer, S.T., Sullivan, M.B., Graham, D.E., Pierce, E.M., Zablocki, O.D., Palumbo, A.V., Elias, D.A., 2019b. Soil Aggregate Microbial Communities: Towards

Understanding Microbiome Interactions at Biologically Relevant Scales. Applied and Environmental Microbiology 85, e00324-19. doi:10.1128/AEM.00324-19
Wood, J.L., Tang, C., Franks, A.E., 2018. Competitive Traits Are More Important than Stress-Tolerance Traits in a Cadmium-Contaminated Rhizosphere: A Role for Trait Theory in Microbial Ecology. Frontiers in Microbiology 9. doi:10.3389/fmicb.2018.00121
Xu, S., Silveira, M.L., Ngatia, L.W., Normand, A.E., Sollenberger, L.E., Ramesh Reddy, K., 2017. Carbon and nitrogen pools in aggregate size fractions as affected by sieving method and land use intensification. Geoderma 305, 70–79. doi:10.1016/j.geoderma.2017.05.044
Yao, J., Rock, C.O., 2017. Exogenous fatty acid metabolism in bacteria. Biochimie 141, 30–39. doi:10.1016/j.biochi.2017.06.015

6. Appendix

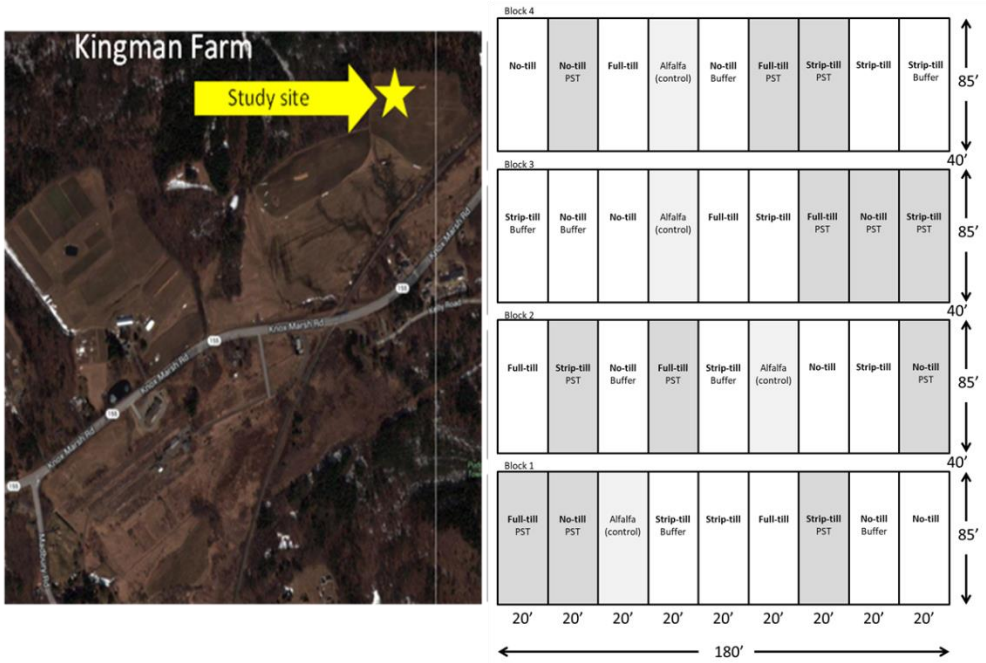

Figure S1: Left: Aerial photograph showing the layout of Kingman Farm (left). The till/pst study plots are located in the upper right of the property. Right: layout of blocks/plots in the till-pst study site. Blocks are 85’ long with 40’ mowed strips separating them. Color designates pesticide seed treatment (PST). White= No-PST; Grey= PST; NT= No-Till, FT= Full-Till, ST= Strip-Till, A= Alfalfa (unsampled ctrl)

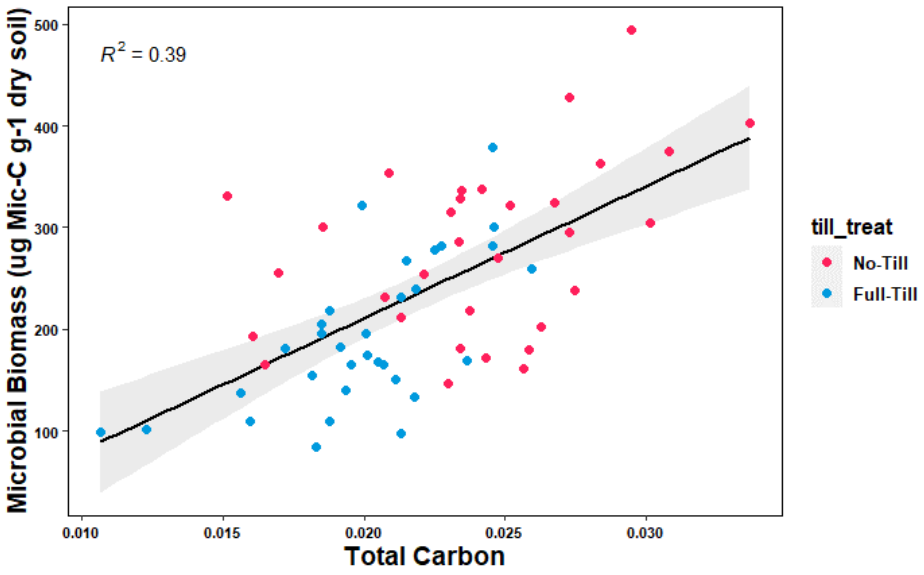

Figure S2: Linear regression of microbial biomass calculated via glucose respiration with the equation from Anderson and Domsch, 1978 against total carbon. Linear modeling determined that the variables were significantly correlated P<0.001.

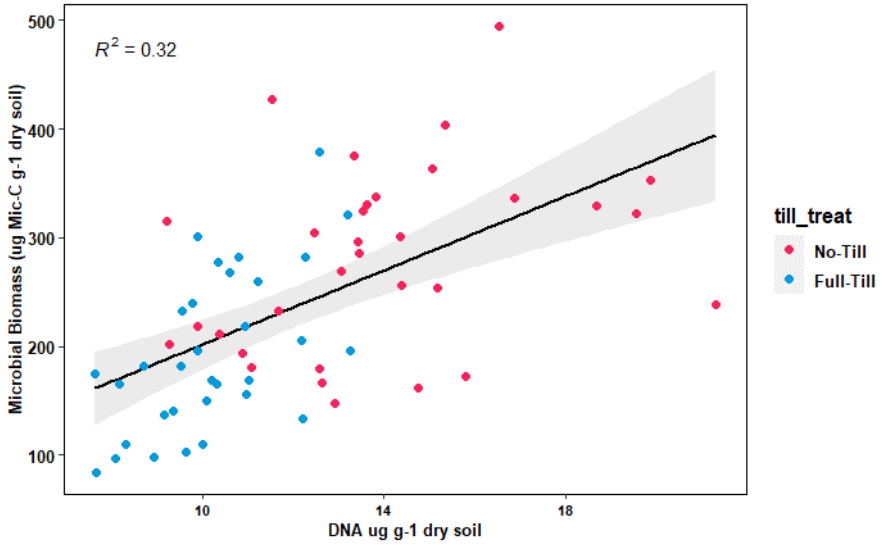

Figure S3: Linear regression of microbial biomass against soil DNA measured as ng DNA per g dry soil. Biomass calculated via glucose respiration with the equation from Anderson and Domsch. Linear modeling determined that the variables were significantly correlated P<0.001.

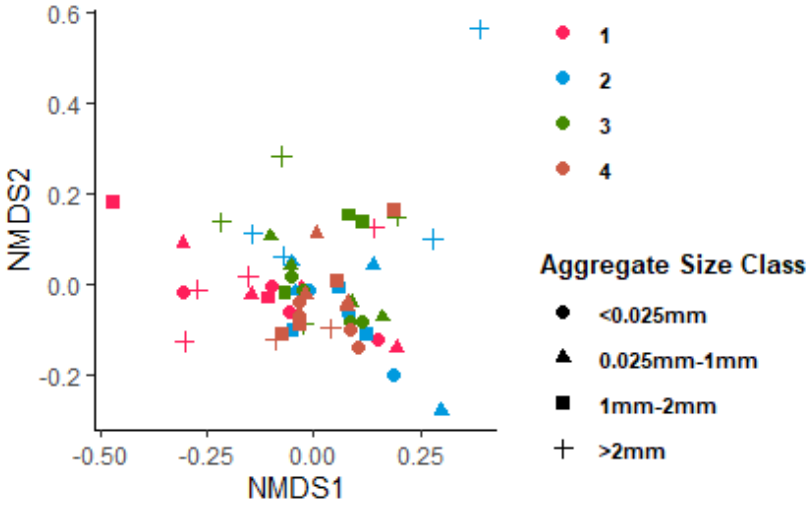

Figure S4: NMDS of 16S bacterial community analyzed at the OTU level colored by block. Bacterial communities in block 1 were significantly different than any other block and as such, PERMANOVA permutations were constrained by block to account for this random effect

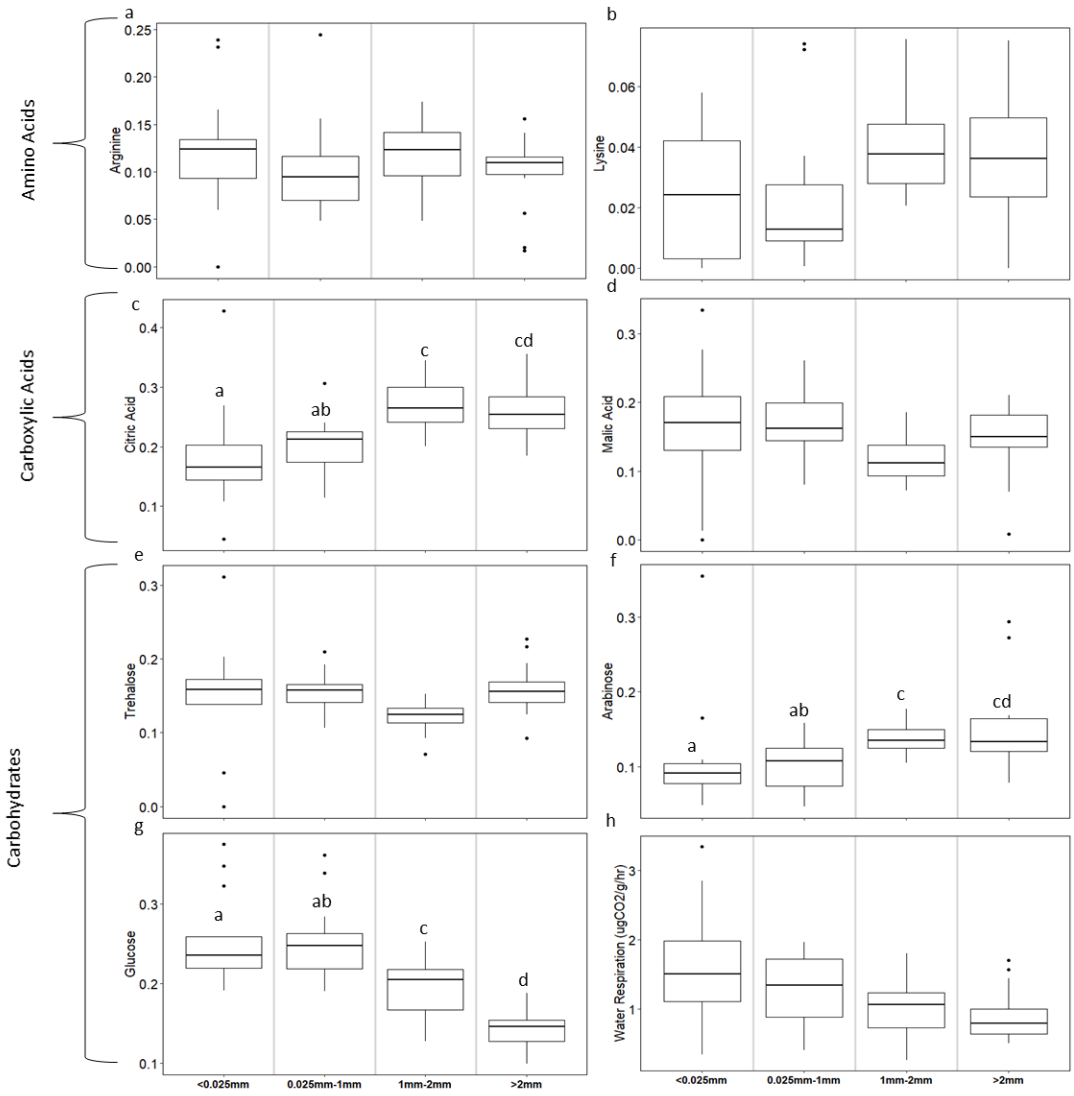

Figure S5: Microbial substrate preference in each aggregate size class. X-axis is proportional substrate contribution to total respiration (panel a-g). Mean values in each aggregate size class sum to 1. Panel h depicts basal respiration in each aggregate size class. TukeyHSD pairwise test confirmed significant differences between respiration in aggregate size classes. Letters denote significance.

Table S1: Community weighted NSTI values for samples included in Picrust2 analysis. Lower NSTI values indicate samples with good reference representation. NSTI values between 0.06 < NSTI < 0.15 are considered good values. Any OTU's with NSTI > 2 standard deviations from mean were discarded from analysis. After quality control, 8149 OTU's were retained.

sample	**weighted_NSTI**
LB_16S_1	0.081055
LB_16S_2	0.093029
LB_16S_3	0.085708
LB_16S_4	0.096764
LB_16S_5	0.110303
LB_16S_6	0.102728
LB_16S_7	0.10931
LB_16S_8	0.095926
LB_16S_10	0.112773
LB_16S_11	0.106172
LB_16S_12	0.097453
LB_16S_14	0.105701
LB_16S_15	0.109831
LB_16S_16	0.099343
LB_16S_18	0.094098
LB_16S_19	0.094662
LB_16S_20	0.094207
LB_16S_21	0.118401
LB_16S_22	0.101297
LB_16S_23	0.107071
LB_16S_24	0.094269
LB_16S_25	0.10373
LB_16S_26	0.098978
LB_16S_27	0.112357
LB_16S_28	0.101437
LB_16S_29	0.110311
LB_16S_30	0.103154
LB_16S_31	0.104774
LB_16S_32	0.067374
LB_16S_34	0.098465
LB_16S_35	0.101493
LB_16S_36	0.087087
LB_16S_37	0.090882
LB_16S_38	0.089149
LB_16S_39	0.101833
LB_16S_40	0.084779
LB_16S_41	0.112045
LB_16S_42	0.096271

LB_16S_43	0.113692
LB_16S_44	0.122051
LB_16S_45	0.100425
LB_16S_46	0.100742
LB_16S_47	0.110877
LB_16S_48	0.094318
LB_16S_49	0.115414
LB_16S_50	0.093069
LB_16S_51	0.097761
LB_16S_53	0.09217
LB_16S_54	0.1118
LB_16S_55	0.107273
LB_16S_57	0.104035
LB_16S_58	0.099947
LB_16S_59	0.106719
LB_16S_60	0.105085
LB_16S_61	0.097653
LB_16S_62	0.101817
LB_16S_63	0.103257
LB_16S_64	0.106076